Evolutionary Dynamics of Variable Games in Structured Populations

Bin Pi, *Student Member, IEEE*, Minyu Feng, *Senior Member, IEEE*, Liang-Jian Deng, *Senior Member, IEEE*, Xiaojie Chen, and Attila Szolnoki

***Abstract*—The game interactions among individuals in nature are often uncertain and dynamically evolving, significantly influencing the persistence of cooperation. However, it remains a formidable challenge to effectively characterize these dynamic properties in structured populations, derive theoretical conditions for cooperation, and identify the optimal game distribution for promoting cooperation. To address these issues, we propose the variable game framework in a structured population, where the game interactions between different individuals change over time. By means of the Markov chain and the pair approximation method, we derive theoretical conditions under which cooperation is favored by natural selection and when it is favored over defection under weak selection. Furthermore, we, respectively, formulate and solve two optimization problems to determine the optimal game distribution that most effectively fosters the evolution of cooperation by maximizing the gradient of cooperation selection and minimizing the fitness difference between defectors and cooperators. The theoretical predictions regarding both the conditions for cooperation and optimal game distribution are further validated by numerical calculations and extensive Monte Carlo simulations. Our findings offer novel insights into the mechanisms driving cooperative behavior in complex systems and provide theoretical guidance for designing optimal game environments that facilitate the evolution of cooperation.**

***Index Terms*—Cooperation, evolutionary dynamics, structured populations, variable game.**

I. Introduction

COOPERATIVE behavior is ubiquitous in nature manifesting on various scales [1], [2], [3], [4], [5] from the synergistic interactions between cells that maintain homeostasis and ensure overall health, to the sophisticated cooperative hunting strategies employed by orcas, which leverage strength and intelligence to capture larger prey, an ability that contributes to their status as apex predators. However, cooperation is often undermined by conflicts of interest among individuals, leading rational agents to favor defection strategies, ultimately resulting in the breakdown of cooperative systems. Consequently, understanding the persistence and evolution of widespread cooperation in nature has drawn considerable attention from researchers across multiple disciplines, including computer science [6], [7], mathematics [8], [9], biology [10], [11], psychology [12], [13], and so on [14], [15], [16].

The integration of complex networks and evolutionary game theory has led to networked evolutionary games, providing a powerful framework for addressing this problem [17], [18], [19]. In this framework, complex networks characterize the structural relationships among individuals in nature, playing a crucial role in the dissemination of information and behaviors, whereas evolutionary game theory captures the dynamics of individual strategy selection and enables the analysis of the evolutionary trends of group behavior. Since the pioneering work of Nowak and May [20] in which they introduced the prisoner's dilemma game on a square lattice network with periodic boundaries, intensive research activity has explored the evolutionary outcomes of various game models (e.g., the snowdrift game [21], [22], [23], the stag-hunt game [24], [25], [26], and public goods game [27], [28], [29]) on different types of complex networks (e.g., small-world networks [30], [31], [32], scale-free networks [33], [34], [35], and temporal networks [36], [37], [38]).

However, it is noteworthy that most previous studies assume a static game interaction in which individuals engage in the same game from the outset [39], [40], [41], [42]. This assumption is idealized, as the game interactions in the real world are often uncertain and dynamically evolving. Feng et al. [43] noticed this and introduced a game transition mechanism based on a Markov process to model the continuously changing psychology of individuals in nature, demonstrating through simulations that such transitions significantly influence the evolution of cooperative behavior. Besides, Hilbe et al. [44] studied a scenario in which the availability of public resources depends on individuals' strategic choices, employing stochastic and evolutionary game theory to show that the dependence of public resources on prior interactions substantially enhances cooperative tendencies. These findings highlight the importance of studying the effects of stochastic and

Received 7 November 2025; revised 22 February 2026; accepted 10 March 2026. Date of publication 23 March 2026; date of current version 20 July 2026. This work was supported in part by the National Natural Science Foundation of China (NSFC) under Grant 12271083, Grant 62273077, and Grant 62473081; in part by the Project of the Department of Science and Technology of Sichuan Province under Grant 2025YFNH0001; and in part by the National Research, Development and Innovation Office (NKFIH) under Grant K142948. This article was recommended by Associate Editor Y. Yuan. *(Corresponding authors: Liang-Jian Deng; Xiaojie Chen.)*

Bin Pi and Xiaojie Chen are with the School of Mathematical Sciences, University of Electronic Science and Technology of China, Chengdu 611731, China (e-mail: xiaojiechen@uestc.edu.cn).

Minyu Feng is with the College of Artificial Intelligence, Southwest University, Chongqing 400715, China.

Liang-Jian Deng is with the School of Mathematical Sciences and the Multi-Hazard Early Warning Key Laboratory of Sichuan Province, University of Electronic Science and Technology of China, Chengdu 611731, China (e-mail: liangjian.deng@uestc.edu.cn).

Attila Szolnoki is with the Institute of Technical Physics and Materials Science, Centre for Energy Research, 1525 Budapest, Hungary.

This article has supplementary material provided by the authors and color versions of one or more figures available at https://doi.org/10.1109/TCYB.2026.3674776.

Digital Object Identifier 10.1109/TCYB.2026.3674776

dynamic game interactions on the emergence and evolution of cooperation.

Although previous studies have explored games with uncertainty in individual interactions, they have primarily relied on Monte Carlo simulations or assumed that the game being played is directly influenced by individuals' strategic choices. For example, Benko et al. [45] introduced the concept of social dilemma transitions to model the evolving dilemmas faced by open data managers, finding that these transitions significantly impact cooperative behavior in open data management through extensive simulations. Additionally, Su et al. [46] examined a framework in which individuals' behaviors and the game played at a given time step influence the game to be played in the subsequent step, revealing that game transitions can serve as a driving force to promote pro-social behavior in highly connected populations. However, there remains a notable gap in the theoretical analysis of game transitions, where the game interactions between individuals dynamically change over time, rather than being related to the behavior of individuals. Furthermore, it is of particular interest to investigate which conditions are most conducive to the emergence of cooperation in the context of game transitions.

To address the aforementioned problem, in this article, we propose the variable game, where the game played between individuals is variable and dynamically evolves over time, a process that can be understood as the durations of different games played between individuals can obey various probability distributions. Our motivation for introducing this framework is to capture game variations influenced by external factors such as seasonal changes or market cycles. For instance, in the case of bulk commodities such as corn, the market dynamics shifts with the seasons. Specifically, during the summer harvest period, supply exceeds demand, placing buyers in a relatively advantageous position and driving market prices downward. Conversely, in winter, when corn supply declines, suppliers gain a competitive advantage, leading to an increase in market prices. Although this framework can be interpreted as a form of game transition, it differs fundamentally from previous studies in which game transitions are primarily driven by individual strategic choices [44], [46]. Specifically, the main contributions of our work are summarized as follows.

1) We propose a novel framework of variable games in which the game interaction between different individuals evolves dynamically over time. Based on this framework, we theoretically derive the conditions under which cooperation is favored by natural selection and when it is favored over defection in a structured population.
2) We obtain the stationary game distribution of interactions between individuals based on the Markov chain and identify the optimal game distribution that facilitates the evolution of cooperation by maximizing the gradient of cooperation selection and minimizing the fitness difference between defectors and cooperators.
3) We conduct numerical calculations and extensive Monte Carlo simulations to validate the theoretical predictions concerning both the conditions under which cooperation is favored by natural selection and when it is favored over defection, as well as the optimal game distribution. Our results demonstrate a strong consistency between theoretical analysis and simulation outcomes.

The rest of this article is structured as follows. In Section II, we first introduce the evolutionary dynamics of variable games and perform theoretical analysis under weak selection to derive the conditions under which cooperation is favored by natural selection and when it is favored over defection. Subsequently, in Section III, we build two different optimization problems from distinct perspectives and theoretically determine the optimal game distribution that best promotes the evolution of cooperation. Then, we present the results of numerical calculations and Monte Carlo simulations to validate our theoretical findings in Section IV. Finally, Section V concludes this article and provides directions for future research.

II. Evolutionary Dynamics of Variable Games

In this section, we investigate the evolutionary dynamics of variable games in structured populations. We begin by outlining the game model and the strategy update rule employed by the population. Subsequently, using the pair approximation method, we derive the theoretical conditions under which cooperative behavior is favored by natural selection and when it is favored over defection.

A. Game Model and Strategy Update

We study the behavioral evolution in a population in which individuals adopt cooperative or defective strategies. The population structure is modeled as a regular network in which each individual is connected to k other neighbors [46], [47], [48]. Each individual occupies a node in the network, and the edges represent game interactions, biological reproduction, or behavioral imitation processes. At each time step, each individual interacts with its neighbors in a game. It is worth noting that the game played between an individual and a neighbor is not fixed; instead, the duration of each game interaction is governed by a random variable with an arbitrary distribution. Once the allotted time for a game elapses, it switches to another game state. This means that there exists a stationary game distribution to determine the game interaction between individuals. We denote the probability that an individual plays game $G_i \in \{G_1, G_2, \ldots, G_n\}$ with a neighbor as π_i, where $\sum_{i=1}^{n} \pi_i = 1$. In other words, an individual can engage in different games with different neighbors.

In this article, we primarily focus on the two-player two-strategy game as the paradigmatic model, which is widely studied in previous research [19], [49]. When the game played between individuals is G_i, interactions between different strategy pairs result in distinct payoffs; mutual cooperation (defection) yields a payoff of $R_i(P_i)$ to both individuals, while cooperation–defection interactions bring a payoff of S_i to the cooperator and T_i to the defector. By introducing the concept of dilemma strength [50], [51], we can denote the payoff matrix of the game G_i played between individuals as

$$M_i = \begin{pmatrix} R_i & P_i - Dr_i \\ R_i + Dg_i & P_i \end{pmatrix} \tag{1}$$

where Dg_i indicates the gamble-intending dilemma and we have $Dg_i = T_i - R_i$, whereas Dr_i represents the risk-averting dilemma and we have $Dr_i = P_i - S_i$. The gamble-intending (Dg_i) and risk-averting (Dr_i) dilemmas measure the extent to which individuals tend to exploit each other and the degree to which they should avoid exploitation, respectively. However, if the values of $R_i - P_i$ are significantly larger than those of Dg_i and Dr_i, resulting in a situation similar to the limit where $T_i \to R_i$ and $P_i \to S_i$, the payoffs for each individual become independent of their own strategy choice and are instead entirely determined by the strategies of their neighbors. To address this issue, we assign $R_i = 1$ and $P_i = 0$, indicating the scaled value for the best reward and the harshest punishment, respectively. Additionally, we constrain both Dg_i and Dr_i within the range of $[-1, 1]$, ensuring a proportional relationship among $R_i - P_i$, Dg_i, and Dr_i. Under these conditions, the evolutionary dynamics depend on the sign and relative magnitude of Dg_i and Dr_i. Therefore, for all games $G_i \in \{G_1, G_2, \ldots, G_n\}$, the payoff matrix is given by

$$M_i = \begin{pmatrix} 1 & -Dr_i \\ 1 + Dg_i & 0 \end{pmatrix} \tag{2}$$

where $Dg_i, Dr_i \in [-1, 1]$. When both Dg_i and Dr_i are positive (negative), the game G_i can be regarded as a prisoner's dilemma game (harmony game). If Dg_i is positive (negative) and Dr_i is negative (positive), the game G_i is classified as a snowdrift game (stag-hunt game). After each individual interacts with all its neighbors in the specific game, it accumulates a total payoff F, calculated as

$$F = \sum_{y \in \Omega} s^T M_y s_y \tag{3}$$

where $s = (1, 0)^T$ and $s = (0, 1)^T$ denote cooperative and defective strategies, respectively. Here, Ω represents the neighborhood set of the focal individual, and M_y indicates the payoff matrix of the game played between the focal individual and its neighbor y. The accumulated payoff is then mapped to the individual's fitness according to the following rule:

$$f = 1 - \omega + \omega F \tag{4}$$

where ω indicates the intensity of selection. We particularly focus on the scenario of weak selection, i.e., $\omega \ll 1$, since the game has only a small effect on individual fitness or it is only one of many factors that influence individual fitness [52], [53], which is widely utilized in evolutionary biology [54].

Next, we consider the strategy update of individuals using the death–birth updating process [55], [56]. In particular, after each individual gets its fitness by interacting with its neighbors, one individual from the population is randomly selected to die. Subsequently, the neighbors of the dead individual occupy the empty site with a probability proportional to their fitness.

B. Evolutionary Dynamics of Cooperation

In this section, we study the conditions under which cooperation is favored by natural selection and when it is favored over defection in structured populations with variable games based on the pair approximation method [57], [58]. We assume that the game between individuals is not deterministic but obeys a certain distribution, and there are two strategies A and B available to all individuals in the population, where A and B can be treated as cooperative and defective behaviors of individuals, respectively.

Theorem 1: For a sufficiently large population size N, we obtain the condition under which natural selection favors strategy A, namely, when the fixation probability of a single A-individual in a population of $N - 1$ B-individuals, denoted by ρ_A, satisfies $\rho_A > 1/N$. This condition can be expressed as follows:

$$3k > \left(2k^2 - 2k - 1\right) \sum_{i=1}^{n} \pi_i Dr_i + \left(k^2 - k + 1\right) \sum_{i=1}^{n} \pi_i Dg_i. \tag{5}$$

Remark 1: The proof is given in Section I of the Supplementary Material. This theorem establishes the condition under which natural selection favors cooperation in a sufficiently large population by comparing the fixation probability of a single cooperator with that under neutral drift. The inequality demonstrated in (5) captures the joint effect of the network structure, characterized by degree k, and the expected payoffs across multiple games in the variable game, weighted by the game distribution π_i. In particular, the coefficients $2k^2 - 2k - 1$ and $k^2 - k + 1$ highlight how network topology can amplify or attenuate the effects of payoff. This result suggests that for cooperation to successfully invade, the weighted average of the gamble-intending dilemma $\sum \pi_i Dg_i$ must be sufficiently low, or similarly, the weighted average of the risk-averting dilemma $\sum \pi_i Dr_i$ must be sufficiently small. Consequently, (5) offers a theoretical guideline for designing cooperative environments. By appropriately adjusting the game distribution in variable games, it is possible to steer the evolutionary dynamics in favor of cooperation.

In the case of a static (nonvariable) game, the condition in (5) reduces to $3k > (2k^2 - 2k - 1)Dr + (k^2 - k + 1)Dg$. Within the framework of the donation game, where a cooperator incurs a cost c to provide a benefit b for the opponent, whereas a defector bears no cost and provides no benefit, we obtain $Dg = Dr = c/(b - c)$. Substituting this into the static-game condition yields the classic rule "$b/c > k$," originally proposed by Ohtsuki et al. [57].

It is important to emphasize that natural selection favoring cooperation does not imply that cooperation is favored over defection. Therefore, we need to make a further derivation for the condition under which cooperation is favored over defection, as established in the following theorem.

Theorem 2: For a sufficiently large population size N, we derive the condition for strategy A to be favored over strategy B, i.e., $\rho_A > \rho_B$, where ρ_B is the fixation probability of a single B-individual in a population of $N - 1$ A-individuals. The corresponding condition is given by

$$\sum_{i=1}^{n} \pi_i \left(Dr_i + Dg_i\right) < \frac{2}{k - 1}. \tag{6}$$

Remark 2: The proof is provided in Section II of the Supplementary Material. This theorem offers a concise and

insightful criterion to determine when cooperation is favored over defection in structured populations. In contrast to Theorem 1, which examines the condition under which natural selection favors cooperation by considering the fixation probability of a single mutant cooperator, Theorem 2 addresses a different condition, i.e., cooperation is more likely to dominate the population than defection. The inequality shown in (6) establishes a direct relationship between the sum of gamble-intending and risk-averting dilemmas $Dr_i + Dg_i$, weighted by the game distribution π_i, and the network connectivity k. The threshold $2/(k-1)$ reflects that higher connectivity requires more stringent conditions to achieve cooperation. This result further underscores the dual influence of network topology and game environment in variable games on evolutionary outcomes. From a practical perspective, these findings offer guidance for designing multigame environments. By properly tuning the game distribution in variable games such that the weighted average payoff remains below a critical threshold, we can foster the prevalence of cooperation over defection.

In the case of a static (nonvariable) game, the condition in (6) transforms into $(Dr + Dg) < 2/(k-1)$. Under the framework of the donation game, where $Dg = Dr = c/(b-c)$, the condition for cooperation to be favored over defection simplifies to "$b/c > k$," which is consistent with the conclusion reached by Ohtsuki et al. [57].

This ends our theoretical analysis of evolutionary dynamics under the proposed variable game framework. Theorems 1 and 2 provide the theoretical conditions under which natural selection favors cooperation and when cooperation can be favored over defection, respectively, if game interactions between individuals are not fixed, but there is a game distribution. To further explore how cooperative behavior can emerge and be sustained, in Sections III, we develop and solve the optimization problem from two distinct perspectives, aiming to identify the optimal game distribution that most promotes the evolution of cooperation in structured populations.

III. Optimal Game Distribution

In real-world scenarios, the game environment in which individuals interact can profoundly shape individual behavior and consequently influence the emergence and evolution of cooperation within a population [45], [59]. Under the variable game framework introduced in this study, different game distributions can yield distinct evolutionary outcomes. Therefore, it is meaningful to identify the optimal game distribution that most effectively facilitates the evolution and persistence of cooperation in structured populations. To do that, we formulate and analyze the optimization problem from two complementary theoretical perspectives, including: 1) maximizing the gradient of cooperation selection and 2) minimizing the fitness difference between defectors and cooperators. These two approaches provide distinct, yet converging insights into how the structure of the game environment can be strategically adjusted to foster cooperative behavior in structured populations.

A. Maximizing the Gradient of Cooperation Selection

Similar to the concept of replicator dynamics in the well-mixed population, the evolutionary dynamics of cooperation characterize the direction and rate of cooperative evolution in the structured population. Based on (13) and (23) of the Supplementary Material, we can obtain the gradient of cooperation selection $\dot{p}_A$ as a function of the percentage of cooperators p_A as

$$\dot{p}_A = \omega \frac{k-2}{k(k-1)} p_A (1-p_A) \times \left[k - \left(k^2-k-1\right) \sum_{i=1}^{n} \pi_i Dr_i - \sum_{i=1}^{n} \pi_i Dg_i + \left(k^2-k-2\right) p_A \sum_{i=1}^{n} \pi_i (Dr_i - Dg_i) \right]. \quad (7)$$

Consequently, cooperative behavior can be promoted by maximizing the gradient of cooperation selection when the gamble-intending and risk-averting dilemmas are sufficiently small. We stress that the term $\omega(k-2)/(k(k-1))p_A(1-p_A)$ is independent of the game distribution and remains positive for $p_A \in (0,1)$ and $k \geq 3$. Therefore, to determine the optimal game distribution that maximizes the gradient of cooperation selection, we formulate the following optimization problem:

$$\begin{aligned} &\max H_1(\Pi) \\ &\text{s.t. } \dot{p}_A = \omega F_1\left(p_A, q_{A|A}\right) \end{aligned} \quad (8)$$

where

$$H_1(\Pi) = -\left(k^2-k-1\right) \sum_{i=1}^{n} \pi_i Dr_i - \sum_{i=1}^{n} \pi_i Dg_i + \left(k^2-k-2\right) p_A \sum_{i=1}^{n} \pi_i (Dr_i - Dg_i).$$

It is worth noting that the game distribution $\Pi = (\pi_1, \pi_2, \ldots, \pi_n)$ varies with the proportion of cooperators p_A. We derive the optimal game distribution that maximizes the gradient of cooperation selection under two different games, as summarized in the following theorem.

Theorem 3: Consider the optimization problem involving two different games. The optimal game distribution Π^* that maximizes the gradient of cooperation selection for any proportion of cooperators is characterized as follows.

1) When $Dr_1 + Dg_2 > Dg_1 + Dr_2$:

1) If $(k^2-k-1)(Dr_1 - Dr_2) + (Dg_1 - Dg_2) < 0$, then the optimal game distribution is $\Pi^* = (1,0)$ for any $p_A \in (0,1)$.
2) If $(k^2-k-1)(Dg_1 - Dg_2) + (Dr_1 - Dr_2) > 0$, then the optimal game distribution is $\Pi^* = (0,1)$ for any $p_A \in (0,1)$.
3) If $(k^2-k-1)(Dr_1 - Dr_2) + (Dg_1 - Dg_2) > 0$ and $(k^2-k-1)(Dg_1 - Dg_2) + (Dr_1 - Dr_2) < 0$, then the optimal game distribution is

$$\Pi^* = \begin{cases} (0,1), & p_A \in \left(0, p_A^*\right) \\ (1,0), & p_A \in \left[p_A^*, 1\right) \end{cases} \quad (9)$$

where $p_A^* = [(k^2 - k - 1)(Dr_1 - Dr_2) + (Dg_1 - Dg_2)]/[(k^2 - k - 2)(Dr_1 - Dg_1 - Dr_2 + Dg_2)]$.

2) When $Dr_1 + Dg_2 < Dg_1 + Dr_2$:

1) If $(k^2 - k - 1)(Dr_1 - Dr_2) + (Dg_1 - Dg_2) > 0$, then the optimal game distribution is $\Pi^* = (0, 1)$ for any $p_A \in (0, 1)$.
2) If $(k^2 - k - 1)(Dg_1 - Dg_2) + (Dr_1 - Dr_2) < 0$, then the optimal game distribution is $\Pi^* = (1, 0)$ for any $p_A \in (0, 1)$.
3) If $(k^2 - k - 1)(Dr_1 - Dr_2) + (Dg_1 - Dg_2) < 0$ and $(k^2 - k - 1)(Dg_1 - Dg_2) + (Dr_1 - Dr_2) > 0$, then the optimal game distribution is

$$\Pi^* = \begin{cases} (1, 0), & p_A \in \left(0, p_A^*\right) \\ (0, 1), & p_A \in \left[p_A^*, 1\right). \end{cases} \tag{10}$$

Remark 3: The proof is given in Section III of the Supplementary Material. This theorem provides a comprehensive characterization of the optimal game distribution that maximizes the gradient of cooperation selection for different proportions of cooperators. A key finding is the optimal game distribution governed by the sign of a specific combination of game parameters, which implies that even minor differences between Dr_i and Dg_i can substantially alter the optimal strategy. In the hybrid case, the presence of a critical threshold p_A^* marks a transition point in the population composition at which the optimal game distribution must be adjusted to maintain the highest selective advantage for cooperation. This underscores the importance of dynamically tuning the game environment in response to the evolving state of the population.

B. Minimizing the Fitness Difference Between Defectors and Cooperators

Next, we aim to facilitate the evolution of cooperative behavior in structured populations by minimizing the fitness difference between defectors and cooperators. This optimization problem is motivated by the crucial role that fitness plays in strategy evolution, and if defectors exhibit higher fitness than cooperators, then defectors are more likely to persist and dominate the population. Therefore, it is meaningful to explore an optimal game distribution that minimizes the fitness difference between defectors and cooperators, thereby fostering cooperative behavior when gamble-intending and risk-averting dilemmas are relatively small. Before that, we need to derive the expected fitness of cooperators $\overline{f_A}$ and defectors $\overline{f_B}$. In a structured population with a regular network, the expected fitness of cooperators $\overline{f_A}$ can be expressed as

$$\begin{aligned} \overline{f_A} = {} & p_B (1 - \omega) \\ & + p_B \omega \left[- \left((k-1) q_{B|A} + 1 \right) \sum_{i=1}^{n} \pi_i Dr_i + (k-1) q_{A|A} \right] \\ & + p_A \omega \left[- (k-1) q_{B|A} \sum_{i=1}^{n} \pi_i Dr_i + \left((k-1) q_{A|A} + 1 \right) \right] \\ & + p_A (1 - \omega) \end{aligned} \tag{11}$$

and the expected fitness of defectors $\overline{f_B}$ is given by

$$\begin{aligned} \overline{f_B} = {} & p_B (1 - \omega) + p_B \omega \left[(k-1) q_{A|B} \left(1 + \sum_{i=1}^{n} \pi_i Dg_i \right) \right] \\ & + p_A \omega \left[\left((k-1) q_{A|B} + 1 \right) \left(1 + \sum_{i=1}^{n} \pi_i Dg_i \right) \right] \\ & + p_A (1 - \omega) \end{aligned} \tag{12}$$

where p_B is the fraction of defectors and $q_{X|Y}$ indicates the conditional probability of finding a neighbor whose strategy is X given that the individual's strategy is Y.

Therefore, to determine the optimal game distribution that minimizes the fitness difference between defectors and cooperators, we can formulate the optimization problem as follows:

$$\begin{aligned} & \min H_2 (\Pi) = \overline{f_B} - \overline{f_A} \\ & \text{s.t. } \dot{p}_A = \omega F_1 \left(p_A, q_{A|A} \right). \end{aligned} \tag{13}$$

We stress that the game distribution $\Pi = (\pi_1, \pi_2, \ldots, \pi_n)$ varies with the frequency of cooperators p_A. In what follows, we derive the optimal game distribution that minimizes the fitness difference between defectors and cooperators under two different games, and the result is summarized in the following theorem.

Theorem 4: Consider the optimization problem involving two different games. The optimal game distribution Π^* that minimizes the fitness difference between defectors and cooperators for any fraction of cooperators is characterized as follows.

1) When $Dg_1 + Dr_2 > Dg_2 + Dr_1$:

1) If $Dr_1 > Dr_2$, then the optimal game distribution is $\Pi^* = (0, 1)$ for any $p_A \in (0, 1)$.
2) If $Dg_1 < Dg_2$, then the optimal game distribution is $\Pi^* = (1, 0)$ for any $p_A \in (0, 1)$.
3) If $Dr_1 < Dr_2$ and $Dg_1 > Dg_2$, then the optimal game distribution is

$$\Pi^* = \begin{cases} (1, 0), & p_A \in \left(0, p_A^*\right) \\ (0, 1), & p_A \in \left[p_A^*, 1\right) \end{cases} \tag{14}$$

where $p_A^* = (Dr_2 - Dr_1)/(Dg_1 - Dg_2 - Dr_1 + Dr_2) \in (0, 1)$.

2) When $Dg_1 + Dr_2 < Dg_2 + Dr_1$:

1) If $Dr_1 < Dr_2$, then the optimal game distribution is $\Pi^* = (1, 0)$ for any $p_A \in (0, 1)$.
2) If $Dg_1 > Dg_2$, then the optimal game distribution is $\Pi^* = (0, 1)$ for any $p_A \in (0, 1)$.
3) If $Dr_1 > Dr_2$ and $Dg_1 < Dg_2$, then the optimal game distribution is

$$\Pi^* = \begin{cases} (0, 1), & p_A \in \left(0, p_A^*\right) \\ (1, 0), & p_A \in \left[p_A^*, 1\right). \end{cases} \tag{15}$$

Remark 4: The proof is provided in Section IV of the Supplementary Material. This theorem characterizes the optimal game distribution that minimizes the fitness difference between defectors and cooperators across all population compositions. The result highlights the sensitivity of the optimal game distribution to the underlying gamble-intending and

risk-averting dilemmas. Interestingly, specific scenarios also give rise to a threshold p_A^*, indicating a critical composition of cooperators in the population at which the system must switch its game distribution to sustain the smallest possible fitness disparity. Notably, this threshold depends solely on the payoff parameters Dr_i and Dg_i, suggesting that effective adaptive control strategies can be devised to facilitate the emergence of cooperative behavior, even in the absence of detailed knowledge about the network structure.

This concludes our theoretical analysis of the optimal game distribution under the variable game framework. Theorems 3 and 4 jointly reveal two complementary design principles for steering evolutionary dynamics toward cooperative behavior. Theorem 3 aims to enhance the directionality of natural selection in favor of cooperation by maximizing the gradient of cooperation selection, whereas Theorem 4 focuses on reducing the advantage of defectors by minimizing the fitness difference between defectors and cooperators.

IV. Numerical and Simulation Results

In this section, we provide a detailed description and analysis of the simulation details as well as the numerical and simulation results to verify our theorems. In particular, in Section IV-A, we first illustrate the simulation methods involved in this article. Following this, we carry out a series of simulations to verify the theoretical conditions for cooperation under the assumption of known stationary distributions of variable games and probability distributions governing game durations, as detailed in Section IV-B. Then, in Section IV-C, we perform numerical calculations and extensive Monte Carlo simulations to validate the theoretical results derived from the optimization problems.

A. Methods

To validate our theoretical findings, we consider the case where the transition occurs between two different games, denoted by G_1 and G_2. Concretely, the duration of each game interaction is not fixed, but follows an arbitrary probability distribution. The game played between individuals changes once the time for the current game has elapsed. The game interaction between individuals i and j can thus be modeled as the Markov chain $\{X_{ij}(t), t \geq 0\}$ with the state space $E = \{G_1, G_2\}$. We assume that the durations for which individuals engage in games G_1 and G_2 are governed by arbitrary distributions $g_1(t)$ and $g_2(t)$, respectively, and that the game interaction between individuals transitions to another game immediately upon the conclusion of the current one. We can get the stationary distribution of individuals playing different games based on the Markov chain theory. Specifically, the probability that the game played between individuals is G_1 can be expressed as

$$\pi_1 = \frac{E\left(T_{G_1}\right)}{E\left(T_{G_1}\right) + E\left(T_{G_1}\right)} = \frac{\int_0^{+\infty} t g_1(t) dt}{\int_0^{+\infty} t\left[g_1(t) + g_2(t)\right] dt} \tag{16}$$

where $E(T_{G_i})$ represents the expected time of game interaction G_i.

Similarly, the probability that the game played between individuals is G_2 is given by

$$\pi_2 = \frac{E\left(T_{G_2}\right)}{E\left(T_{G_1}\right) + E\left(T_{G_1}\right)} = \frac{\int_0^{+\infty} t g_2(t) dt}{\int_0^{+\infty} t\left[g_1(t) + g_2(t)\right] dt}. \tag{17}$$

By substituting the derived values of π_1 and π_2 into (5) and (6), we can obtain the theoretical conditions under which natural selection favors cooperation and cooperation can be favored over defection when the distribution governing game duration is known.

Algorithm 1 Simulation of Fixation Probability

Initialize the total number of simulations *num*, the current simulation count $run = 0$, the counter for successful fixations of cooperators num_C (defectors num_D), and the regular network structure $\mathcal{G}$, where each individual is connected to k neighbors. All individuals are initially assigned to defect D (cooperate C).
while $run < num$ **do**
  Randomly select one individual i from the population and set $s_i \leftarrow C$ ($s_i \leftarrow D$) as the invading strategy.
  while the population has not reached an absorbing state **do**
    Randomly select one individual j to be replaced.
    One of j's neighbors is selected to reproduce and fill the vacancy, with a probability proportional to their fitness.
    if All individuals are cooperators (defectors) **then**
      $num_C(num_D) \leftarrow num_C(num_D) + 1$.
      $run \leftarrow run + 1$.
      Break.
    end if
    if All individuals are defectors (cooperators) **then**
      $run \leftarrow run + 1$.
      Break.
    end if
  end while
end while
Compute the fixation probability of cooperation (defection): $\rho_C(\rho_D) \leftarrow \frac{num_C(num_D)}{num}$.

The population structure is modeled as a square lattice with periodic boundaries using von Neumann neighborhoods (where each individual has four neighbors, i.e., $k = 4$) or Moore neighborhoods (where each individual has eight neighbors, i.e., $k = 8$). To simulate the fixation probability ρ_C (ρ_D) of cooperation (defection), we initialize the population with only defectors (cooperators) and randomly select one individual to adopt the opposite strategy as an invader. The simulation proceeds until the population reaches one of the two absorbing states, i.e., all individuals in the population are either cooperators or defectors. The fixation probability ρ_C (ρ_D) is then calculated as the proportion of simulations in which a single cooperator (defector) successfully takes over the entire population, based on 5×10^5 independent Monte Carlo simulations. The detailed simulation procedure for computing the fixation probability is presented in Algorithm 1.

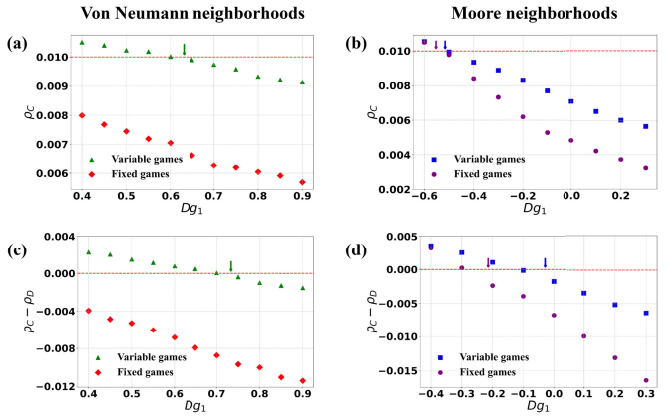

Fig. 1. Fixation probability of evolutionary dynamics with known game distributions. This figure shows ρ_C and $\rho_C - \rho_D$ as functions of Dg_1 under different regular networks and game distributions. The arrows in the first and second rows indicate the theoretical conditions under which natural selection favors cooperation ($\rho_C > 1/N$) and cooperation is favored over defection ($\rho_C > \rho_D$) in different scenarios, respectively. The horizontal red dashed line represents the neutral drift, corresponding to (a) and (b) $\rho_C = 1/N$ and (c) and (d) $\rho_C = \rho_D$.

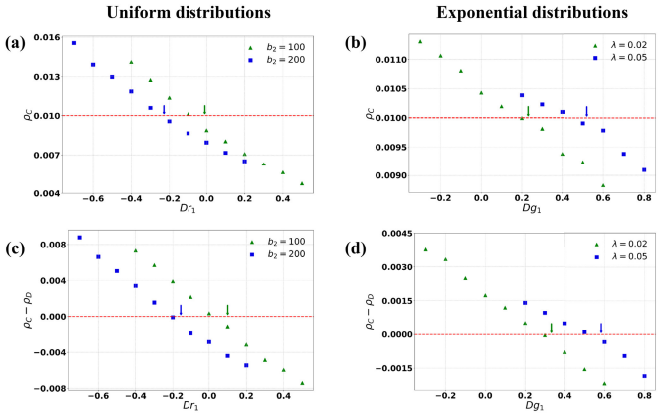

Fig. 2. Fixation probability of evolutionary dynamics with the same probability distributions governing the durations of different games. The first and second columns show the evolution of fixation probability under uniform and exponential distributions, respectively. The panels in the first row show the variation of ρ_C, while those in the second row discuss $\rho_C - \rho_D$. The green and blue arrows indicate the theoretical conditions for cooperation to be favored by natural selection ($\rho_C > 1/N$) and cooperation to be favored over defection ($\rho_C > \rho_D$) under different transition rates, respectively. The horizontal red dashed line denotes the baseline for neutral drift, corresponding to (a) and (b) $\rho_C = 1/N$ and (c) and (d) $\rho_C = \rho_D$.

B. Evolution of Cooperation With Variable Games

In this section, we consider the scenario in which the stationary distribution of transitions between two different games, G_1 and G_2, is known and denoted by π_1 and π_2, respectively. To verify the theoretical predictions regarding the evolution of cooperation under given stationary distributions demonstrated in Theorems 1 and 2, we conduct different simulations on square lattice networks with von Neumann neighborhoods ($k = 4$) and Moore neighborhoods ($k = 8$), respectively, where the network size is fixed at $N = 100$. The corresponding results are presented in Fig. 1, which depicts ρ_C and $\rho_C - \rho_D$ as functions of Dg_1 under different network structures and stationary distributions. The variable game scenario corresponds to the distribution $\pi_1 = 0.5$ and $\pi_2 = 0.5$, while the fixed game scenario corresponds to $\pi_1 = 1.0$ and $\pi_2 = 0.0$. The arrows indicate the theoretical thresholds derived from (5) and (6), representing the conditions under which natural selection favors cooperation and cooperation is favored over defection, respectively, across different regular networks and stationary distributions. The red horizontal line marks the baseline of neutral drift for reference.

From Fig. 1, we clearly observe that both the fixation probability of cooperation ρ_C and the difference $\rho_C - \rho_D$ decrease with an increase in the payoff parameter Dg_1. This is because an increase in Dg_1 leads to a greater fitness for defectors, which in turn reduces the number of cooperators in the population. In addition, by comparing the simulation results with the theoretical critical values, we find that they are in relatively good agreement. Specifically, when the payoff parameter Dg_1 is less than the theoretical value marked by the arrow, the cooperation shown in Fig. 1(a) and (b) can be favored by natural selection, i.e., $\rho_C > 1/N$, and the cooperation illustrated in Fig. 1(c) and (d) is favored over defection, i.e., $\rho_C - \rho_D > 0$. Furthermore, we find that the points labeled by green triangles in Fig. 1(a) and (c) are always above the red diamonds in the square lattice network with periodic boundaries using von Neumann neighborhoods. This suggests that the introduction of variable games better facilitates the emergence and maintenance of cooperation compared to the evolution of cooperation in fixed games. In the case of Moore's neighborhoods presented in Fig. 1(b) and (d), we can obtain the same conclusion. Moreover, by comparing the theoretical thresholds of variable and fixed games marked by the arrows, we find that the blue arrow is always to the right of the purple arrow, indicating that variable games can facilitate the evolution of cooperation more than fixed games, consistent with the results observed under the von Neumann neighborhoods.

In what follows, we consider the scenario in which the stationary distribution of transitions between two different games is unknown; instead, only the probability distributions governing the durations of different games are specified. Fig. 2 depicts the results of the fixation probability when the durations of both games obey uniform or exponential distributions. The first and second columns correspond separately to the uniform and exponential cases, while the first and second rows illustrate how ρ_C and $\rho_C - \rho_D$ vary with respect to the payoff parameters, respectively.

The results across all four panels in Fig. 2 consistently show that the simulation outcomes align well with the theoretical predictions and that cooperation will be inhibited as the payoff parameters Dr_1 and Dg_1 increase, since higher values of these parameters improve the fitness of defectors. Further comparisons under different duration distributions yield a deeper insight. In particular, when the durations of game interactions follow a uniform distribution, where the time to play G_i obeys the uniform distribution of a_i to b_i, i.e., $T_{G_i} \sim U(a_i, b_i)$, the results shown in Fig. 2(a) and (c) are obtained on the lattice network of size $N = 100$ with Moore neighborhoods. The parameters related to the durations are set as $a_1 = a_2 = 50$ and $b_1 = 150$, and those related to the payoffs are fixed at

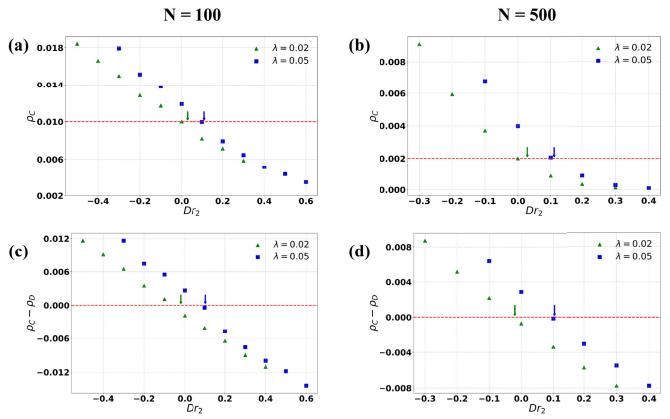

Fig. 3. Fixation probability of evolutionary dynamics with arbitrary probability distributions governing the durations of different games. The first and second rows illustrate ρ_C and $\rho_C - \rho_D$ against Dr_2 under different exponential transition rates. The first column corresponds to a network size of $N = 100$, while the second column shows the results for $N = 500$. The green and blue arrows denote the theoretical thresholds under which natural selection favors cooperation ($\rho_C > 1/N$) and cooperation can be favored over defection ($\rho_C > \rho_D$) at transition rates $\lambda = 0.02$ and $\lambda = 0.05$, respectively. The horizontal red dashed line represents the neutral drift, with $\rho_C = 1/N$ for panels (a) and (b) and $\rho_C = \rho_D$ for panels (c) and (d).

$Dg_1 = -0.2$, $Dg_2 = 0.3$, and $Dr_2 = 0.5$. It can be observed that the point of $b_2 = 100$ marked by the green triangle is always above that of $b_2 = 200$ marked by the blue square, and the green arrow is shifted to the right of the blue, suggesting that lowering b_2, the upper bound of the uniform distribution for G_2, facilitates the evolution of cooperation. This phenomenon arises because G_2 imposes a stronger social dilemma than G_1, and reducing b_2 effectively shortens the average duration of the harsher game. On the other hand, when the game durations follow exponential distributions, where the time to play G_1 and G_2 obeys the exponential distribution of λ and μ, i.e., $T_{G_1} \sim E(\lambda)$ and $T_{G_2} \sim E(\mu)$, the results displayed in Fig. 2(b) and (d) are obtained on the lattice network of size $N = 100$ with von Neumann neighborhoods. The transition rate from G_2 to G_1 is fixed at $\mu = 0.02$, and the payoff parameters are set as $Dr_1 = 0.5$, $Dg_2 = 0.2$, and $Dr_2 = 0.3$. In this setting, increasing the transition rate λ from G_1 to G_2 favors the survival of the cooperators. This effect can be explained in the same way as for the uniform case: by reducing the average duration spent in the more challenging game environment, the evolutionary pressure on cooperators is alleviated.

Next, we explore the case where the durations for individuals to engage in games obey arbitrary, potentially distinct distributions. Unlike the previous case illustrated in Fig. 2, where both games shared the same type of distribution, here we assume that the time to play G_1 follows an exponential distribution with parameter λ, i.e., $T_{G_1} \sim E(\lambda)$, while the time to play game G_2 follows a uniform distribution over the interval $[a, b]$, i.e., $T_{G_2} \sim U(a, b)$. It is also worth noting that previous simulations were conducted on networks of size $N = 100$. In this analysis, we also examine the impact of a larger network, specifically a square lattice with $N = 500$. The parameters associated with the payoffs are set as $Dg_1 = 0.5$, $Dg_2 = 0.1$, and $Dr_1 = 0.3$. The first and second rows of Fig. 3 depict the evolution of ρ_C and $\rho_C - \rho_D$ as a function of the payoff parameter Dr_2 for various values of the transition rate λ under network sizes of $N = 100$ and $N = 500$, respectively. We emphasize that the level of neutral drift, indicated by the red horizontal dashed line in Fig. 3(a) and (b), differs due to the distinct network sizes.

As shown in Fig. 3, the simulation results are in good agreement with the theoretical predictions for both network sizes, $N = 100$ and $N = 500$. It is evident that cooperation is increasingly suppressed as the payoff parameter Dr_2 increases. Moreover, we observe that a higher transition rate λ promotes the evolution of cooperation. Specifically, the data point corresponding to $\lambda = 0.05$, indicated by the blue square, consistently lies above the one for $\lambda = 0.02$, marked by the green triangle. Similarly, the theoretical threshold represented by the blue arrow is always greater than that indicated by the green arrow. This observation can be explained by the fact that the social dilemma in game G_2 is weaker than that in G_1. Therefore, increasing the transition rate λ shortens the duration of G_1 and effectively extends the time individuals spend playing G_2, which is more conducive to the persistence of cooperation. These findings are consistent with the results presented in Fig. 2(b) and (d).

C. Numerical Calculations and Monte Carlo Results for Optimization

In this section, we validate the theoretical results of the optimal game distribution derived in Section III through numerical calculations and Monte Carlo simulations.

1) Numerical and Simulation Results for Maximizing the Gradient of Cooperation Selection: To verify the theoretical results concerning the maximization of the gradient of cooperation selection illustrated in Theorem 3, we present the numerical results of the gradient of cooperation selection as a function of the cooperator proportion, as well as the corresponding evolutionary trajectories of cooperator frequency over time, shown in the first and second columns of Fig. 4, respectively. We emphasize that the numerical calculation of the temporal evolution of cooperation frequency in the second column is governed by the differential equation presented in (7). Consequently, the corresponding evolutionary trajectories are deterministic. Our results indicate that an evolution time of $t = 10\,000$ is sufficient to reveal the superiority of the optimal game distribution over other game distributions. Additionally, the third column of Fig. 4 displays Monte Carlo simulation results for the evolution of cooperator frequency over time. We note that the results in the third column are obtained from Monte Carlo simulations, which inherently introduce stochasticity into the strategy updating process at each step. Therefore, the corresponding evolutionary trajectories are nondeterministic. Since the strategy update follows a death–birth process, in which only one individual updates its strategy per time step, a sufficiently long evolutionary timescale is required to capture the asymptotic behavior of the system. Our simulations show that when the evolutionary time is set to $t = 1\,00\,000$, the optimal game distribution exhibits a distinct advantage over other game distributions. The parameter configurations for rows 1–3 in Fig. 4 satisfy the condition $Dg_2 + Dr_1 > Dg_1 + Dr_2$, with $(k^2 - k - 1)(Dr_1 - Dr_2) + (Dg_1 - Dg_2) < 0$ for

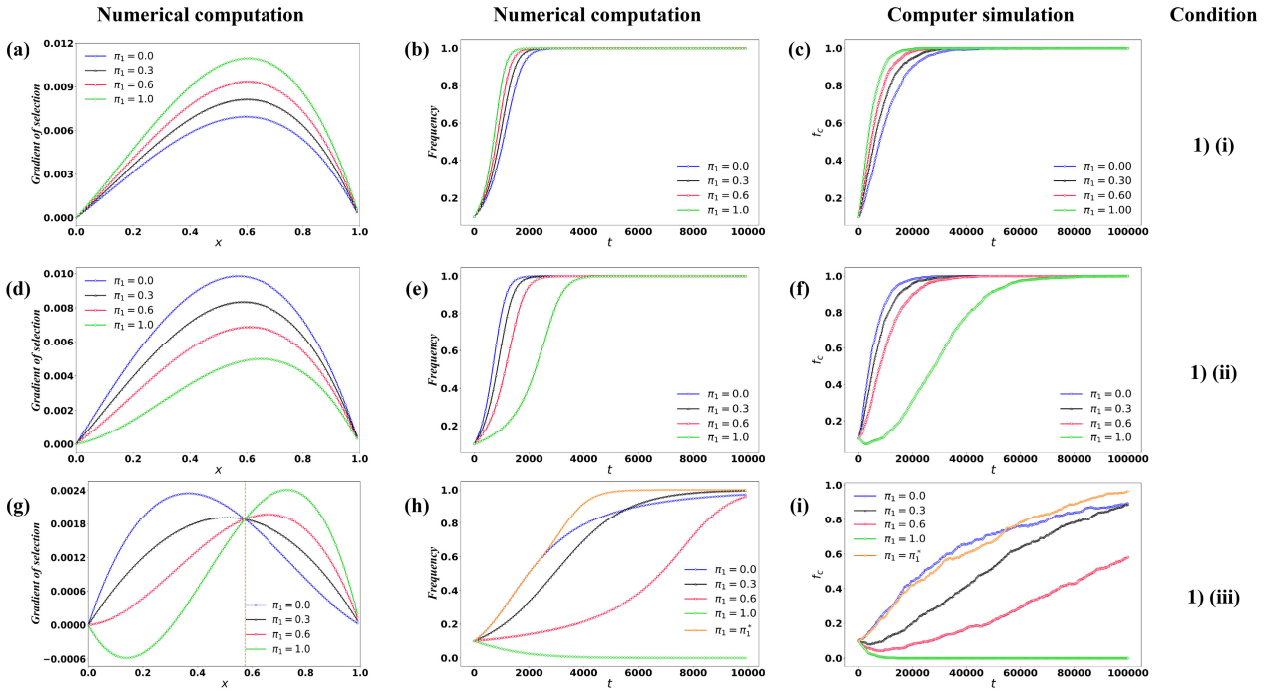

Fig. 4. Numerical and simulation results for maximizing the gradient of cooperation selection. The first column panels (a), (d), and (g) illustrates the numerical results of the gradient of cooperation selection as a function of the fraction of cooperators under different stationary game distributions. The second panels (b), (e), and (h) and third panels (c), (f), and (i) columns display the corresponding numerical and Monte Carlo simulation results, respectively, for the evolutionary trajectories of the cooperator frequency over time. Each row corresponds to a different theoretical case for maximizing the gradient of cooperation selection, as stated in items (i)–(iii) of Theorem 3. The vertical orange dashed line in (g) denotes the critical point x^* at which $G_1(x^*) = 0$ shown in (33) of the Supplementary Material.

row 1, $(k^2 - k - 1)(Dg_1 - Dg_2) + (Dr_1 - Dr_2) > 0$ for row 2, and $(k^2 - k - 1)(Dr_1 - Dr_2) + (Dg_1 - Dg_2) > 0, (k^2 - k - 1)(Dg_1 - Dg_2) + (Dr_1 - Dr_2) < 0$ for row 3.

In Fig. 4(a), we find that the gradient of selection corresponding to $\pi_1 = 1.0$ marked by green diamonds is the highest across all values of cooperator frequency and decreases monotonically as π_1 decreases. Furthermore, the result presented in Fig. 4(b) shows that all scenarios eventually reach the pure cooperator state, with $\pi_1 = 1.0$ achieving this outcome the fastest. As π_1 decreases, the time required to reach full cooperation increases. The Monte Carlo simulation results in Fig. 4(c) corroborate these findings. In contrast, in Fig. 4(d), we find that the gradient of selection is maximized for $\pi_1 = 0.0$ marked by the blue circles and decreases as π_1 increases. Fig. 4(e) further confirms that cooperation emerges most rapidly when $\pi_1 = 0.0$, compared to other situations. These observations are again supported by the simulation results illustrated in Fig. 4(f). In Fig. 4(g), a threshold phenomenon is observed. When the cooperator frequency $x \in (0, x^*]$, where $x^* = [(k^2 - k - 1)(Dr_1 - Dr_2) + (Dg_1 - Dg_2)]/[(k^2 - k - 2)(Dr_1 - Dg_1 - Dr_2 + Dg_2)]$, indicated by the orange vertical dashed line, the gradient of selection is largest for $\pi_1 = 0.0$; however, when $x \in (x^*, 1)$, the gradient of selection is maximized for $\pi_1 = 1.0$. Furthermore, both the numerical and simulation results presented in Fig. 4(h) and (i) demonstrate that, given a sufficiently long evolutionary time, the cooperator frequency under $\pi_1 = \pi_1^*$ always achieves the highest or reaches the full cooperation state fastest compared to the other cases, where π_1^* denotes the value of π_1 that maximizes the gradient of selection in Fig. 4(g). These results strongly validate the theoretical predictions, with both numerical and simulation outcomes displaying excellent agreement. Additionally, we verify the remaining three theoretical cases in the Supplementary Material, and the interested readers can refer to Section V-A of the Supplementary Material for further details. These results also support the same conclusion: the numerical and simulation outcomes are in excellent agreement with the theoretical predictions.

2) Numerical and Simulation Results for Minimizing the Fitness Difference Between Defectors and Cooperators: To verify the theoretical prediction of minimizing the fitness difference between defectors and cooperators shown in Theorem 4, we present the numerical results of the fitness difference with respect to the proportion of cooperators, along with the evolution of the cooperator frequency over time based on (7). These results are separately illustrated in the first and second columns of Fig. 5. Moreover, the third column of Fig. 5 displays the Monte Carlo simulation results depicting the temporal evolution of the cooperator frequency. The evolutionary time for the numerical calculation and computer simulation of the cooperation ratio in the second and third columns is set to $t = 10\,000$ and $t = 100\,000$, respectively. These settings are sufficient to clearly capture the advantage of the optimal game distribution over other game distributions in promoting cooperation. The parameter settings for rows 1–3 in Fig. 5 all satisfy $Dg_1 + Dr_2 > Dg_2 + Dr_1$, with specific distinctions as follows: row 1 corresponds to $Dr_1 > Dr_2$, row 2 corresponds

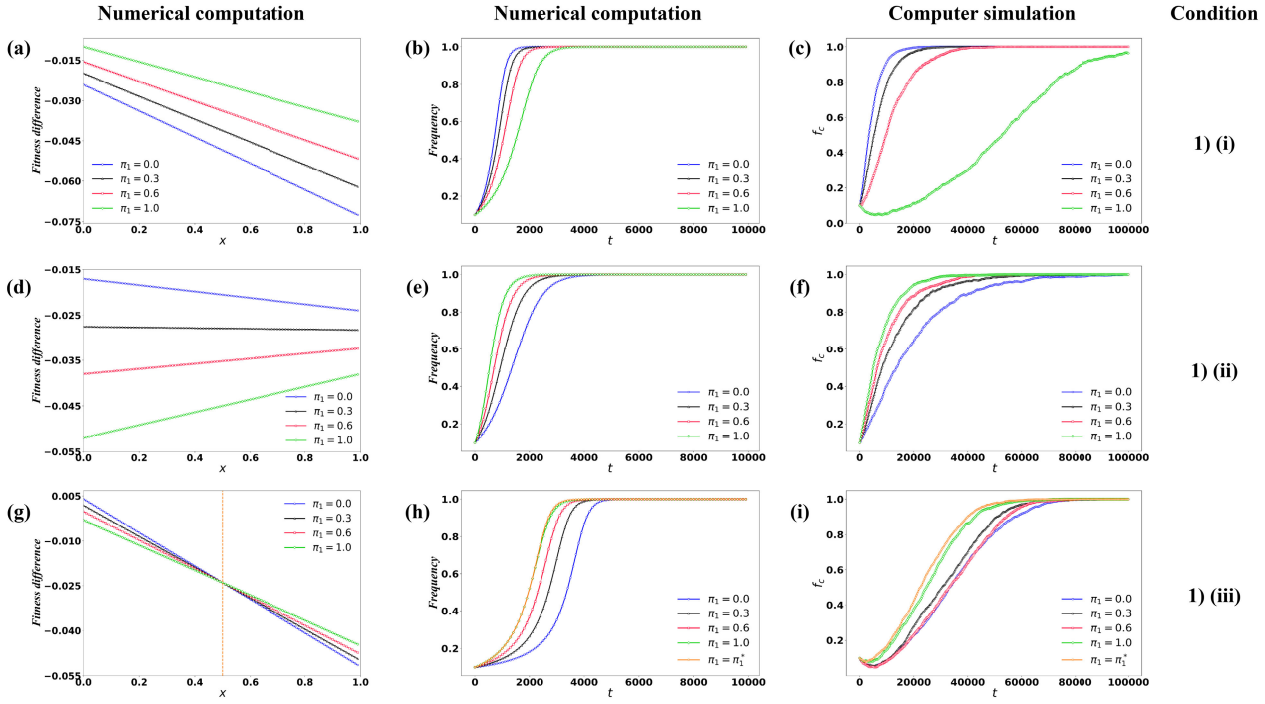

Fig. 5. Numerical and simulation results for minimizing the fitness difference between defectors and cooperators. The first column panels (a), (d), and (g) represents the numerical results of the fitness difference between defectors and cooperators as a function of the proportion of cooperators under different stationary game distributions. The second panels (b), (e), and (h) and third panels (c), (f), and (i) columns display the numerical and simulation results, respectively, for the evolutionary trajectories of the cooperator frequency over time under these distributions. Each row corresponds to a different theoretical case for minimizing the fitness difference between defectors and cooperators, as described in items (i)–(iii) of Theorem 4. The orange vertical dashed line in (g) indicates the critical point x^* that makes $G_2(x^*) = 0$ presented in (37) of the Supplementary Material.

to $Dg_1 < Dg_2$, and row 3 corresponds to $Dr_1 < Dr_2$ and $Dg_1 > Dg_2$.

In Fig. 5(a), we observe that the fitness difference between defectors and cooperators is minimized at $\pi_1 = 0.0$ marked by blue circles and grows as π_1 increases. In addition, Fig. 5(b) demonstrates that all scenarios eventually reach the fully cooperative state, with $\pi_1 = 0.0$ achieving it the fastest. The speed to reach full cooperation decreases as π_1 increases for the other scenarios. These findings are corroborated by the Monte Carlo simulation results displayed in Fig. 5(c). It is worth noting that the discrepancies between the numerical calculation and computer simulation of cooperative evolution in Fig. 5(b) and (c) are natural. This is because the numerical result is obtained from (7), which describes a deterministic evolutionary process, whereas the computer simulation is obtained through Monte Carlo simulation, which inherently involves stochasticity in individual strategy updates, leading to indeterminate evolutionary trajectories. In Fig. 5(d), we find that the fitness difference is minimized for $\pi_1 = 1.0$ indicated by green diamonds and increases as π_1 decreases. Analogously, Fig. 5(e) demonstrates that the fully cooperative state is reached most rapidly when $\pi_1 = 1.0$, a conclusion also supported by the simulation results shown in Fig. 5(f). In Fig. 5(g), we identify a critical threshold $x^* = (Dr_2 - Dr_1)/(Dg_1 - Dg_2 - Dr_1 + Dr_2)$ marked by the orange vertical dashed line. When the cooperator frequency $x \in (0, x^*]$, the fitness difference is smallest for $\pi_1 = 1.0$; in contrast, for $x \in (x^*, 1)$, the smallest fitness difference occurs at $\pi_1 = 0.0$. Furthermore, the numerical and simulation results depicted in Fig. 5(h) and (i) reveal that over a sufficiently long evolution period, the scenario with $\pi_1 = \pi_1^*$ achieves the highest number of cooperators or reaches full cooperation the fastest compared to the other cases, where π_1^* corresponds to the value of π_1 that minimizes the fitness difference in Fig. 5(g). All of these results support strong agreement between theoretical predictions and both numerical and simulation outcomes. Furthermore, the remaining three theoretical cases are validated in the Supplementary Material. Interested readers are referred to Section V-B of the Supplementary Material for detailed discussions. These additional results further confirm that the numerical and simulation outcomes are in excellent agreement with the theoretical predictions.

V. Conclusion and Discussion

In this article, we studied the two-player two-strategy evolutionary dynamics in structured populations under the proposed variable game framework, where the game interactions between individuals are not fixed, different from the common assumption in traditional models. In contrast, the durations of different game interactions follow a certain distribution, and we can obtain the stationary distribution of individuals engaged in various games. Based on the pair approximation method, we derived the theoretical conditions under which cooperation can be favored by natural selection and when it is favored over defection in structured populations. Notably, by applying our conclusions for the static (nonvariable) game to the donation game, we recovered the classic rule "$b/c > k$"

[57], thereby validating the theoretical framework. To verify our theoretical results, we focused on the representative case involving transitions between two different games and performed extensive Monte Carlo simulations. The results demonstrated strong consistency between theoretical predictions and the simulation outcomes. The comparative analysis further revealed that the proposed variable game promotes cooperative behavior more effectively than the fixed game. In addition, we explored the model's robustness by conducting simulations across different neighborhood configurations and network sizes in regular graphs. In all cases, the results remain consistent with the theoretical expectations, highlighting the robustness and generality of the proposed framework.

We also formulated two optimization problems in terms of: 1) maximizing the gradient of cooperation selection and 2) minimizing the fitness difference between defectors and cooperators. Through rigorous theoretical analysis, we derived the corresponding optimal game distribution that most effectively promotes the evolution of cooperation. To validate these theoretical findings, we performed numerous numerical calculations and Monte Carlo simulations for each optimization scenario. The obtained results showed that both the numerical and simulation results are in good agreement with the theoretical predictions. It is important to note that our theoretical analysis of the optimal game distribution primarily focused on the scenarios involving two distinct games. When the optimization problem extends to three or more games, obtaining an analytical solution becomes substantially more complex. In such cases, the problem can instead be addressed by numerical calculations or computational simulations. Moreover, our findings highlight that the proposed variable game mechanism exerts a substantial impact on both the fixation probability of cooperation and the conditions under which cooperation is most likely to evolve. Our work can offer valuable insights into the design of optimal game environments to foster the emergence and maintenance of cooperative behavior, particularly in contexts where modifying environmental conditions is more feasible than altering individual strategies.

Notably, the proposed variable game mechanism can be regarded as a form of game transition. However, it fundamentally differs from earlier studies, where game transitions are typically driven by individual strategic behaviors [44], [46], whereas the motivation in this article is to model transitions influenced by external factors such as seasonal changes or market cycles. Besides, while [43] and [45] investigated the effects of game transitions on the evolution of cooperation, their analysis was based on simulation experiments exclusively and did not derive the theoretical conditions under which cooperation can be favored over defection. Furthermore, we establish two optimization problems based on maximizing the gradient of cooperation selection and minimizing the fitness difference between defectors and cooperators, and theoretically derive the optimal game distribution that best promotes the evolution of cooperation. This theoretical framework represents a novel contribution, as it has not been addressed in previous works on game transitions.

Within the variable game framework proposed in this article, several intriguing directions merit further investigation. For example, our theoretical analysis is primarily developed for regular networks, whereas population structures often exhibit other properties in reality, such as small-world effects [60], scale-free properties [61], or temporal dynamics [62]. Besides, our research mainly employs two-player games, whereas multiplayer games are also commonly observed in practice, such as public goods games [63]. Therefore, extending the study to these more complex population structures and diverse interaction models is meaningful and remains an important avenue for future research.

REFERENCES

[1] T. Ren and X.-J. Zeng, "Reputation-based interaction promotes cooperation with reinforcement learning," *IEEE Trans. Evol. Comput.*, vol. 28, no. 4, pp. 1177–1188, Aug. 2024.

[2] W. Guan, X. Song, T. Gan, J. Lin, X. Chang, and L. Nie, "Cooperation learning from multiple social networks: Consistent and complementary perspectives," *IEEE Trans. Cybern.*, vol. 51, no. 9, pp. 4501–4514, Sep. 2021.

[3] M. Chica, W. Rand, and F. C. Santos, "The evolution and social cost of herding mentality promote cooperation," *IScience*, vol. 26, no. 10, Oct. 2023, Art. no. 107927.

[4] J. H. Fowler and N. A. Christakis, "Cooperative behavior cascades in human social networks," *Proc. Nat. Acad. Sci. USA*, vol. 107, no. 12, pp. 5334–5338, Mar. 2010.

[5] H. Wei, J. Zhang, C. Zhang, and M. Cao, "Indirect reciprocity enhances collective cooperation on weighted networks," *IEEE Trans. Cybern.*, vol. 56, no. 2, pp. 1141–1152, Feb. 2026.

[6] Z. Zeng, M. Feng, M. Perc, and J. Kurths, "Bursty switching dynamics promotes the collapse of network topologies," *Proc. Roy. Soc. A, Math., Phys. Eng. Sci.*, vol. 481, no. 2310, Mar. 2025, Art. no. 20240936.

[7] H. Tembine, E. Altman, R. El-Azouzi, and Y. Hayel, "Evolutionary games in wireless networks," *IEEE Trans. Syst., Man, Cybern., B (Cybern.)*, vol. 40, no. 3, pp. 634–646, Jun. 2010.

[8] S. Wang, M. Cao, and X. Chen, "Optimally combined incentive for cooperation among interacting agents in population games," *IEEE Trans. Autom. Control*, vol. 70, no. 7, pp. 4562–4577, Jul. 2025.

[9] B. Pi, M. Feng, and L.-J. Deng, "A memory-based spatial evolutionary game with the dynamic interaction between learners and profiteers," *Chaos, Interdiscipl. J. Nonlinear Sci.*, vol. 34, no. 6, Jun. 2024, Art. no. 063120.

[10] M. A. Nowak, "Five rules for the evolution of cooperation," *Science*, vol. 314, no. 5805, pp. 1560–1563, 2006.

[11] C. Kasper et al., "Genetics and developmental biology of cooperation," *Mol. Ecol.*, vol. 26, no. 17, pp. 4364–4377, 2017.

[12] J. Henrich and M. Muthukrishna, "The origins and psychology of human cooperation," *Annu. Rev. Psychol.*, vol. 72, no. 1, pp. 207–240, Jan. 2021.

[13] J. R. Stevens, F. A. Cushman, and M. D. Hauser, "Evolving the psychological mechanisms for cooperation," *Annu. Rev. Ecol., Evol., Systematics*, vol. 36, no. 1, pp. 499–518, Dec. 2005.

[14] Z. Zeng, M. Feng, and A. Szolnoki, "Evolutionary dynamics with self-interaction learning in networked systems," *IEEE Trans. Netw. Sci. Eng.*, vol. 13, pp. 296–313, 2026.

[15] M. Perc, J. Jordan, D. G. Rand, Z. Wang, S. Boccaletti, and A. Szolnoki, "Statistical physics of human cooperation," *Phys. Rep.*, vol. 687, pp. 1–51, May 2017.

[16] Y. Zhang, M. Feng, Q. Li, M. Perc, and A. Szolnoki, "Effects of stochastic games on evolutionary dynamics in structured populations," *Commun. Phys.*, early access, 2026.

[17] V. Vargas-Panesso, N. Quijano, L. F. Giraldo, and J. Barreiro-Gomez, "Modeling strategic intercommunity connections in evolutionary games," *IEEE Trans. Cybern.*, early access, Feb. 6, 2026, doi: 10.1109/TCYB.2026.3655536.

[18] M. Chica, R. Chiong, M. Kirley, and H. Ishibuchi, "A networked *N*-player trust game and its evolutionary dynamics," *IEEE Trans. Evol. Comput.*, vol. 22, no. 6, pp. 866–878, Dec. 2018.

[19] Z. Zeng, M. Feng, P. Liu, and J. Kurths, "Complex network modeling with power-law activating patterns and its evolutionary dynamics," *IEEE Trans. Syst.*, vol. 55, no. 4, pp. 2546–2559, Apr. 2025.

[20] M. A. Nowak and R. M. May, "Evolutionary games and spatial chaos," *Nature*, vol. 359, no. 6398, pp. 826–829, May 1992.

[21] C. Hauert and M. Doebeli, "Spatial structure often inhibits the evolution of cooperation in the snowdrift game," *Nature*, vol. 428, no. 6983, pp. 643–646, Apr. 2004.
[22] K. Li, Y. Mao, Z. Wei, and R. Cong, "Pool-rewarding in N-person snowdrift game," *Chaos, Solitons Fractals*, vol. 143, Feb. 2021, Art. no. 110591.
[23] Y. Zhu, H. Cui, and C. Xia, "Adaptive reputation promotes the cooperation of multiplayer snowdrift game on higher-order networks," *Phys. A, Stat. Mech. Appl.*, vol. 675, Oct. 2025, Art. no. 130824.
[24] Y. Dong, H. Xu, and S. Fan, "Memory-based stag hunt game on regular lattices," *Phys. A, Stat. Mech. Appl.*, vol. 519, pp. 247–255, Apr. 2019.
[25] J. D. Bairagya and S. Chakraborty, "Coordinating cooperation in stag-hunt game: Emergence of evolutionarily stable procedural rationality," *J. Phys., Complex.*, vol. 6, no. 3, Sep. 2025, Art. no. 035004.
[26] Q. Luo, L. Liu, and X. Chen, "Evolutionary dynamics of cooperation in the N-person stag hunt game," *Phys. D, Nonlinear Phenomena*, vol. 424, Oct. 2021, Art. no. 132943.
[27] X. Wang, Z. Yang, G. Chen, and Y. Liu, "Enhancing cooperative evolution in spatial public goods game by particle swarm optimization based on exploration and Q-learning," *Appl. Math. Comput.*, vol. 469, May 2024, Art. no. 128534.
[28] E. Pichler and A. M. Shapiro, "Public goods games on adaptive coevolutionary networks," *Chaos*, vol. 27, no. 7, 2017, Art. no. 073107.
[29] J. Han, B. Pi, X. Chen, and A. Szolnoki, "Public goods cooperation via group interaction with opponent selection," *Chaos, Solitons Fractals*, vol. 199, Oct. 2025, Art. no. 116821.
[30] X. Chen and L. Wang, "Promotion of cooperation induced by appropriate payoff aspirations in a small-world networked game," *Phys. Rev. E, Stat. Phys. Plasmas Fluids Relat. Interdiscip. Top.*, vol. 77, no. 1, Jan. 2008, Art. no. 017103.
[31] X.-H. Deng, Y. Liu, and Z.-G. Chen, "Memory-based evolutionary game on small-world network with tunable heterogeneity," *Phys. A, Stat. Mech. Appl.*, vol. 389, no. 22, pp. 5173–5181, Nov. 2010.
[32] H. Wickramaarachchi and M. Kirley, "Uncertainty driven decision making and perturbation dynamics in evolutionary games on small-world networks," *Phys. A, Stat. Mech. Appl.*, vol. 674, Sep. 2025, Art. no. 130719.
[33] F. C. Santos and J. M. Pacheco, "Scale-free networks provide a unifying framework for the emergence of cooperation," *Phys. Rev. Lett.*, vol. 95, no. 9, Aug. 2005, Art. no. 098104.
[34] A. Szolnoki, M. Perc, and Z. Danku, "Towards effective payoffs in the Prisoner's dilemma game on scale-free networks," *Phys. A, Stat. Mech. Appl.*, vol. 387, nos. 8–9, pp. 2075–2082, Mar. 2008.
[35] T. Konno, "Scale-free networks enhance the spread of better strategy," *Dyn. Games Appl.*, vol. 15, no. 1, pp. 103–128, Mar. 2025.
[36] P. Holme and J. Saramäki, "Temporal networks," *Phys. Rep.*, vol. 519, no. 3, pp. 97–125, 2012.
[37] Z. Zhang, Y. Xia, and Q. Su, "The structure-coefficient theorem for evolutionary games on temporal networks," in *Proc. 44th Chin. Control Conf. (CCC)*, Jul. 2025, pp. 1034–1041.
[38] A. Li et al., "Evolution of cooperation on temporal networks," *Nature Commun.*, vol. 11, no. 1, p. 2259, May 2020.
[39] Y. Zhu, Z. Zhang, C. Xia, X. Li, and Z. Chen, "Finite strategy switches of coordinating and anti-coordinating games on weighted networks," *IEEE Trans. Cybern.*, vol. 56, no. 1, pp. 446–459, Jan. 2026.
[40] Y. Yang and X. Li, "Towards a snowdrift game optimization to vertex cover of networks," *IEEE Trans. Cybern.*, vol. 43, no. 3, pp. 948–956, Jun. 2013.
[41] C. Tang, A. Li, and X. Li, "When reputation enforces evolutionary cooperation in unreliable MANETs," *IEEE Trans. Cybern.*, vol. 45, no. 10, pp. 2190–2201, Oct. 2015.
[42] A. Liu, L. Wang, G. Chen, and X. Guan, "Heterogeneously networked evolutionary games with intergroup conflicts," *IEEE Trans. Cybern.*, vol. 54, no. 10, pp. 5684–5695, Oct. 2024.
[43] M. Feng, B. Pi, L.-J. Deng, and J. Kurths, "An evolutionary game with the game transitions based on the Markov process," *IEEE Trans. Syst., Man, Cybern., Syst.*, vol. 54, no. 1, pp. 609–621, Jan. 2024.
[44] C. Hilbe, Š. Šimsa, K. Chatterjee, and M. A. Nowak, "Evolution of cooperation in stochastic games," *Nature*, vol. 559, no. 7713, pp. 246–249, Jul. 2018.
[45] T. P. Benko, B. Pi, Q. Li, M. Feng, M. Perc, and H. B. Vošner, "Evolutionary games for cooperation in open data management," *Appl. Math. Comput.*, vol. 496, Jul. 2025, Art. no. 129364.
[46] Q. Su, A. McAvoy, L. Wang, and M. A. Nowak, "Evolutionary dynamics with game transitions," *Proc. Nat. Acad. Sci. USA*, vol. 116, no. 51, pp. 25398–25404, 2019.
[47] J. Han, X. Chen, and A. Szolnoki, "When selection pays: Structured public goods game with a generalized interaction mode," *Chaos, Interdiscipl. J. Nonlinear Sci.*, vol. 34, no. 3, Mar. 2024, Art. no. 033124.
[48] Y. Sakamoto and M. Ueda, "Pink-noise dynamics in an evolutionary game on a regular graph," *Phys. Rev. E, Stat. Phys. Plasmas Fluids Relat. Interdiscip. Top.*, vol. 110, no. 3, Sep. 2024, Art. no. 034110.
[49] B. Allen et al., "Evolutionary dynamics on any population structure," *Nature*, vol. 544, no. 7649, pp. 227–230, Apr. 2017.
[50] Z. Wang, S. Kokubo, M. Jusup, and J. Tanimoto, "Universal scaling for the dilemma strength in evolutionary games," *Phys. Life Rev.*, vol. 14, pp. 1–30, Sep. 2015.
[51] M. Fahimur Rahman Shuvo and K. A. Kabir, "Investigating the impact of environmental feedback on the optional Prisoner's dilemma for insights into cyclic dominance and evolution of cooperation," *Roy. Soc. Open Sci.*, vol. 11, no. 10, 2024, Art. no. 240717.
[52] F. Fu, L. Wang, M. A. Nowak, and C. Hauert, "Evolutionary dynamics on graphs: Efficient method for weak selection," *Phys. Rev. E, Stat. Phys. Plasmas Fluids Relat. Interdiscip. Top.*, vol. 79, no. 4, Apr. 2009, Art. no. 046707.
[53] A. McAvoy and B. Allen, "Fixation probabilities in evolutionary dynamics under weak selection," *J. Math. Biol.*, vol. 82, no. 3, p. 14, Feb. 2021.
[54] M. A. Nowak, A. Sasaki, C. Taylor, and D. Fudenberg, "Emergence of cooperation and evolutionary stability in finite populations," *Nature*, vol. 428, no. 6983, pp. 646–650, Apr. 2004.
[55] K. Kaveh, N. L. Komarova, and M. Kohandel, "The duality of spatial death–birth and birth–death processes and limitations of the isothermal theorem," *Roy. Soc. Open Sci.*, vol. 2, no. 4, Apr. 2015, Art. no. 140465.
[56] B. Allen et al., "Transient amplifiers of selection and reducers of fixation for death-birth updating on graphs," *PLOS Comput. Biol.*, vol. 16, no. 1, Jan. 2020, Art. no. e1007529.
[57] H. Ohtsuki, C. Hauert, E. Lieberman, and M. A. Nowak, "A simple rule for the evolution of cooperation on graphs and social networks," *Nature*, vol. 441, no. 7092, pp. 502–505, May 2006.
[58] Z. Sun, X. Chen, and A. Szolnoki, "State-dependent optimal incentive allocation protocols for cooperation in public goods games on regular networks," *IEEE Trans. Netw. Sci. Eng.*, vol. 10, no. 6, pp. 3975–3988, Jun. 2023.
[59] K. Emmerich and M. Masuch, "The impact of game patterns on player experience and social interaction in co-located multiplayer games," in *Proc. Annu. Symp. Comput.-Hum. Interact. Play*, Oct. 2017, pp. 411–422.
[60] D. J. Watts and S. H. Strogatz, "Collective dynamics of 'small-world'networks," *Nature*, vol. 393, no. 6684, pp. 440–442, 1998.
[61] A.-L. Barabási and R. Albert, "Emergence of scaling in random networks," *Science*, vol. 286, no. 5439, pp. 509–512, Oct. 1999.
[62] B. Pi, L.-J. Deng, M. Feng, M. Perc, and J. Kurths, "Dynamic evolution of complex networks: A reinforcement learning approach applying evolutionary games to community structure," *IEEE Trans. Pattern Anal. Mach. Intell.*, vol. 47, no. 10, pp. 8563–8582, Oct. 2025.
[63] J. Shi, C. Liu, and J. Liu, "Hypergraph-based model for modeling multi-agent Q-learning dynamics in public goods games," *IEEE Trans. Netw. Sci. Eng.*, vol. 11, no. 6, pp. 6169–6179, Nov. 2024.

Bin Pi (Student Member, IEEE) received the B.E. degree in data science and big data technology from the College of Artificial Intelligence, Southwest University, Chongqing, China, in 2023. He is currently pursuing the M.S. degree in mathematics with the School of Mathematical Sciences, University of Electronic Science and Technology of China, Chengdu, China.

His research interests include complex networks, evolutionary games, stochastic processes, and reinforcement learning.

Minyu Feng (Senior Member, IEEE) received the joint Ph.D. degree in computer science from the University of Electronic Science and Technology of China, Chengdu, China, and Humboldt University of Berlin, Berlin, Germany, in 2018.

Since 2019, he has been an Associate Professor with the College of Artificial Intelligence, Southwest University, Chongqing, China. He has published more than 80 peer-reviewed articles in authoritative journals, such as IEEE TRANSACTIONS ON PATTERN ANALYSIS AND MACHINE INTELLIGENCE, IEEE TRANSACTIONS ON SYSTEMS, MAN, AND CYBERNETICS: SYSTEMS, and IEEE TRANSACTIONS ON CYBERNETICS. His research interests include complex systems, evolutionary game theory, computational social science, and mathematical epidemiology.

Dr. Feng is a Senior Member of China Computer Federation (CCF) and Chinese Association of Automation (CAA). Currently, he serves as a Subject Editor for *Applied Mathematical Modeling*, an Academic Editor for *PLOS Computational Biology*, an Editorial Advisory Board Member for Chaos, and an Editorial Board Member for *Humanities and Social Sciences Communications*, *Scientific Reports*, and *International Journal of Mathematics for Industry*. Besides, he is a reviewer of Mathematical Reviews of American Mathematical Society.

Liang-Jian Deng (Senior Member, IEEE) received the B.S. and Ph.D. degrees in applied mathematics from the School of Mathematical Sciences, University of Electronic Science and Technology of China (UESTC), Chengdu, China, in 2010 and 2016, respectively.

From 2013 to 2014, he was a joint-training Ph.D. Student with Case Western Reserve University, Cleveland, OH, USA. In 2017, he was a Post-Doctoral Researcher with Hong Kong Baptist University (HKBU), Hong Kong. In addition, he has stayed with the Isaac Newton Institute for Mathematical Sciences, University of Cambridge, Cambridge, U.K., and HKBU, for short visits. He is currently a Professor with the School of Mathematical Sciences, UESTC. His research interests include the use of optimization modeling, deep learning, and numerical PDEs to address several tasks in image processing and computer vision, e.g., resolution enhancement and restoration. Please visit his homepage for more information: https://liangjiandeng.github.io/

Xiaojie Chen received the bachelor's degree from the National University of Defense Technology, Changsha, China, in 2005, and the Ph.D. degree from Peking University, Beijing, China, in 2011.

From September 2008 to September 2009, he was a Visiting Scholar with The University of British Columbia, Vancouver, BC, Canada. From February 2011 to January 2013, he was a Post-Doctoral Research Scholar with the International Institute for Applied Systems Analysis (IIASA), Laxenburg, Austria. From February 2013 to January 2014, he was a Research Scholar with IIASA. He is currently a Professor with the School of Mathematical Sciences, University of Electronic Science and Technology of China, Chengdu, China. He has published over 100 journal articles. His main research interests include evolutionary dynamics, decision-making in game interactions, game-theoretical control, and collective intelligence.

Attila Szolnoki is currently a Research Advisor with the Centre for Energy Research, Budapest, Hungary. He has authored around 200 original research articles with more than 25 000 citations and an H-factor of 83. His current research interests include evolutionary game theory, phase transitions, statistical physics, and their applications.

Dr. Szolnoki is an Outstanding or a Distinguished Referee of several internationally recognized journals. Besides, he serves or has served as an Editor for scientific journals, including *EPL*, *Physica A*, *Scientific Reports*, *Applied Mathematics and Computation*, *Frontiers in Physics*, *PLoS One*, *Entropy*, or *Indian Journal of Physics*. He is among the top 1% most cited physicists according to Thomson Reuters Highly Cited Researchers.

Evolutionary Dynamics of Variable Games in Structured Populations (Supplementary Material)

Bin Pi, Minyu Feng, *Senior Member, IEEE,* Liang-Jian Deng, *Senior Member, IEEE,* Xiaojie Chen, and Attila Szolnoki

***Abstract*—This supplementary material contains the detailed proofs of Theorems 1-4 presented in the main manuscript, along with additional figures that support and complement the main findings related to the optimization analysis.**

***Index Terms*—Evolutionary dynamics, variable game, cooperation, structured populations.**

I. Proof of Theorem 1

We employ the symbols p_A and p_B to denote the proportions of strategies A and B utilized in the population. Let p_{XY} and $q_{X|Y}$ respectively represent the frequency of XY strategy pairs in the system and the conditional probability of finding a neighbor whose strategy is X given that the individual's strategy is Y, where X and Y can be either A or B. Then, we have the following equation holds

$$\begin{cases} p_A + p_B = 1 \\ q_{A|X} + q_{B|X} = 1 \\ p_{XY} = p_X q_{Y|X} \\ p_{XY} = p_{YX} \end{cases}, \tag{1}$$

which suggests that the whole system can be described in terms of the variables p_A and $q_{A|A}$, with all other variables being functions of these two variables. We emphasize that the strategies of individuals in the system evolve dynamically during the evolutionary process, with a primary focus on the frequency of strategy A utilized by individuals. Next, we derive the dynamical equation for the evolution of cooperation in the population and further identify the conditions under which cooperation dominates.

This work was supported in part by the National Natural Science Foundation of China (NSFC) under Grant Nos. 12271083, 62273077, and 62473081, in part by the Project of the Department of Science and Technology of Sichuan Province under Grant No. 2025YFNH0001, and in part by the National Research, Development and Innovation Office (NKFIH) under Grant No. K142948.

Bin Pi and Xiaojie Chen are with the School of Mathematical Sciences, University of Electronic Science and Technology of China, Chengdu 611731, China (e-mail: xiaojiechen@uestc.edu.cn).

Liang-Jian Deng is with the School of Mathematical Sciences & Multi-Hazard Early Warning Key Laboratory of Sichuan Province, University of Electronic Science and Technology of China, Chengdu 611731, China (e-mail: liangjian.deng@uestc.edu.cn).

Minyu Feng is with the College of Artificial Intelligence, Southwest University, Chongqing 400715, China.

Attila Szolnoki is with the Institute of Technical Physics and Materials Science, Centre for Energy Research, P.O. Box 49, H-1525 Budapest, Hungary.

Corresponding authors: Liang-Jian Deng and Xiaojie Chen.

A. Updating a B-individual

We begin by considering the case in which a B-individual is selected to die, and an A-individual from the neighborhood succeeds in reproducing to occupy the position of the dead individual. Suppose that there are k_A A-individuals among the k neighbors of the dead B-individual, then the probability of this particular neighborhood configuration can be expressed as

$$\mathscr{A}(k_A) = \begin{pmatrix} k \\ k_A \end{pmatrix} q_{A|B}^{k_A} q_{B|B}^{k_B}, \tag{2}$$

where k_B is the number of B-individuals among the k neighbors of the dead B-individual, and we have $k_B = k - k_A$.

The fitness of each A-individual that plays the game with the dead B-individual is

$$f_A = 1 - \omega + \omega \left[(k-1)\, q_{A|A} - \left((k-1)\, q_{B|A} + 1 \right) \sum_{i=1}^{n} \pi_i D r_i \right], \tag{3}$$

and the fitness of each B-individual that plays the game with the dead B-individual is

$$f_B = 1 - \omega + \omega \left[(k-1)\, q_{A|B} \left(1 + \sum_{i=1}^{n} \pi_i D g_i \right) \right]. \tag{4}$$

The probability that one of the neighboring A-individuals replaces the dead B-individual can be expressed as

$$P\left(A \to B\right) = \frac{k_A f_A}{k_A f_A + k_B f_B}. \tag{5}$$

Therefore, p_A increases by $1/N$ with probability

$$\begin{aligned} P\left(\Delta p_A = \frac{1}{N}\right) &= p_B \sum_{k_A + k_B = k} \mathscr{A}(k_A) P\left(A \to B\right) \\ &= p_B \sum_{k_A + k_B = k} \frac{k!}{k_A! k_B!} q_{A|B}^{k_A} q_{B|B}^{k_B} \frac{k_A f_A}{k_A f_A + k_B f_B}. \end{aligned} \tag{6}$$

Meanwhile, the success of an A-individual in occupying the position of a dead B-individual leads to an increase in the number of AA-pair in the system by k_A, and thus p_{AA} grows by $k_A/(kN/2)$ with probability

$$\begin{aligned} P\left(\Delta p_{AA} = \frac{2k_A}{kN}\right) &= p_B \mathscr{A}(k_A) P\left(A \to B\right) \\ &= p_B \frac{k!}{k_A! k_B!} q_{A|B}^{k_A} q_{B|B}^{k_B} \frac{k_A f_A}{k_A f_A + k_B f_B}. \end{aligned} \tag{7}$$

B. Updating an A-individual

Subsequently, we consider the situation in which an A-individual is chosen to die, and a B-individual in the neighborhood succeeds in reproducing to occupy the position of the dead individual. We assume that there are k_A A-individuals and k_B B-individuals among the k neighbors of the dead A-individual, where $k_A + k_B = k$, then the probability of this specific neighborhood configuration is given by

$$\mathscr{B}(k_A) = \begin{pmatrix} k \\ k_A \end{pmatrix} q_{A|A}^{k_A} q_{B|A}^{k_B}. \tag{8}$$

The fitness of each A-individual who plays the game with the dead A-individual is

$$g_A = 1-\omega+\omega\left[\left((k-1)\,q_{A|A}+1\right)-(k-1)\,q_{B|A}\sum_{i=1}^{n}\pi_i Dr_i\right], \tag{9}$$

and the fitness of each B-individual who plays the game with the dead A-individual is

$$g_B = 1-\omega+\omega\left[\left((k-1)\,q_{A|B}+1\right)\left(1+\sum_{i=1}^{n}\pi_i Dg_i\right)\right]. \tag{10}$$

The probability that one of the neighboring B-individuals replaces the dead A-individual can be expressed as

$$P\left(B\to A\right) = \frac{k_B g_B}{k_A g_A + k_B g_B}. \tag{11}$$

Therefore, p_A decreases by $1/N$ with probability

$$\begin{aligned} P\left(\Delta p_A = -\frac{1}{N}\right) &= p_A \sum_{k_A+k_B=k} \mathscr{B}(k_A) P\left(B\to A\right) \\ &= p_A \sum_{k_A+k_B=k} \frac{k!}{k_A! k_B!} q_{A|A}^{k_A} q_{B|A}^{k_B} \frac{k_B g_B}{k_A g_A + k_B g_B}. \end{aligned} \tag{12}$$

Simultaneously, the success of a B-individual in occupying the position of a dead A-individual leads to a reduction in the number of AA-pair in the system by k_A. Consequently, p_{AA} reduces by $k_A/(kN/2)$ with probability

$$\begin{aligned} P\left(\Delta p_{AA} = -\frac{2k_A}{kN}\right) &= p_A \mathscr{B}(k_A) P\left(B\to A\right) \\ &= p_A \frac{k!}{k_A! k_B!} q_{A|A}^{k_A} q_{B|A}^{k_B} \frac{k_A g_A}{k_A g_A + k_B g_B}. \end{aligned} \tag{13}$$

C. Evolutionary Dynamics of Cooperation

Hereby, we assume that the death of an individual and the replacement of a neighbor's strategy occur within one unit of time, $1/N$. Then, the derivative of p_A can then be expressed as

$$\begin{aligned} \dot{p}_A &= \left[\frac{1}{N} P\left(\Delta p_A = \frac{1}{N}\right) + \left(-\frac{1}{N}\right) P\left(\Delta p_A = -\frac{1}{N}\right)\right] N \\ &= \omega \frac{k-1}{k} p_{AB} \left(I_a - I_b \sum_{i=1}^{n} \pi_i Dr_i - I_c \sum_{i=1}^{n} \pi_i Dg_i\right) + O\left(\omega^2\right), \end{aligned} \tag{14}$$

where I_a, I_b, and I_c are shown as follows

$$\begin{cases} I_a = (k-1)(q_{A|A}+q_{B|B})(q_{A|A}-q_{A|B}) \\ I_b = (k-1) q_{B|A}(q_{A|A}+q_{B|B}) + q_{B|B} \\ I_c = (k-1) q_{A|B}(q_{A|A}+q_{B|B}) + q_{A|A} \end{cases}. \tag{15}$$

Analogously, we can obtain the time derivative of the fraction of AA-pair, which is given by

$$\begin{aligned} \dot{p}_{AA} &= \left[\sum_{k_A=0}^{k} \frac{2k_A}{kN} P\left(\Delta p_{AA} = \frac{2k_A}{kN}\right) \right. \\ &\quad \left. + \sum_{k_A=0}^{k} \left(-\frac{2k_A}{kN}\right) P\left(\Delta p_{AA} = -\frac{2k_A}{kN}\right)\right] / \left(\frac{1}{N}\right) \\ &= \frac{2}{k} p_{AB} \left[1 + (k-1)\left(q_{A|B} - q_{A|A}\right)\right] + O\left(\omega\right). \end{aligned} \tag{16}$$

Therefore, we can derive the derivative of $q_{A|A}$

$$\begin{aligned} \dot{q}_{A|A} &= \frac{d}{dt}\left(\frac{p_{AA}}{p_A}\right) \\ &= \frac{2}{k} q_{B|A} \left[1 + (k-1)\left(q_{A|B} - q_{A|A}\right)\right] + O\left(\omega\right). \end{aligned} \tag{17}$$

As previously stated, the entire system can be represented solely by p_A and $q_{A|A}$, i.e., Eqs. (14) and (17) can be respectively denoted as

$$\dot{p}_A = \omega F_1\left(p_A, q_{A|A}\right) + O\left(\omega^2\right), \tag{18}$$

and

$$\dot{q}_{A|A} = F_2\left(p_A, q_{A|A}\right) + O\left(\omega\right). \tag{19}$$

When the intensity of selection is weak, i.e., $\omega \ll 1$, the local frequency $q_{A|A}$ achieves equilibrium more rapidly than the global fraction p_A. Consequently, the dynamical system converges swiftly to the slow manifold with $\dot{q}_{A|A} = 0$, and we get

$$q_{A|A} - q_{A|B} = \frac{1}{k-1}. \tag{20}$$

As we mentioned before, the whole system can be represented by p_A and $q_{A|A}$. With the new constraints outlined in Eq. (20), the whole system can subsequently be characterized by a single variable p_A.

D. Diffusion Approximation

Next, we investigate the one-dimensional diffusion process of the random variable p_A. Let Δp_A as a random variable within a very short time interval Δt. The expectation $E[\Delta p_A]$ and variance $V[\Delta p_A]$ of Δp_A can be respectively expressed as

$$\begin{aligned} E\left[\Delta p_A\right] &= \frac{1}{N} P\left(\Delta p_A = \frac{1}{N}\right) + \left(-\frac{1}{N}\right) P\left(\Delta p_A = -\frac{1}{N}\right) \\ &= \omega \frac{k-2}{Nk} p_A \left(1-p_A\right) \left(I_a - I_b \sum_{i=1}^{n} \pi_i Dr_i - I_c \sum_{i=1}^{n} \pi_i Dg_i\right) \Delta t \\ &\equiv m\left(p_A\right) \Delta t, \end{aligned} \tag{21}$$

and

$$\begin{aligned} V\left[\Delta p_A\right] &= E\left[\Delta^2 p_A\right] - E^2\left[\Delta p_A\right] \\ &= \frac{2\left(k-2\right)}{N^2\left(k-1\right)} p_A\left(1-p_A\right)\Delta t \equiv v\left(p_A\right)\Delta t, \end{aligned} \tag{22}$$

where $m(p_A)$ and $v(p_A)$ are the mean and variance of the increment of p_A with a very short time interval Δt. Combining Eqs. (1) and (20), and substituting the values of $q_{A|A}, q_{B|B}, q_{A|B}, q_{B|A}$ obtained from the solution into Eq. (15), we yield

$$\begin{cases} I_a = \frac{k}{k-1} \\ I_b = \frac{k^2-k-1-\left(k^2-k-2\right)p_A}{k-1} \\ I_c = \frac{1+\left(k^2-k-2\right)p_A}{k-1} \end{cases}. \tag{23}$$

The fixation probability $\phi_A(x)$ of the A-individual with initial ratio $p_A(t=0)=x$ follows the differential equation:

$$m\left(x\right)\frac{d\phi_A\left(x\right)}{dx} + \frac{v\left(x\right)}{2}\frac{d^2\phi_A\left(x\right)}{dx^2} = 0, \tag{24}$$

and by solving Eq. (24), we have

$$\phi_A\left(x\right) = \frac{\int_0^x \varphi\left(y\right)dy}{\int_0^1 \varphi\left(y\right)dy}, \tag{25}$$

where $\varphi\left(y\right) = e^{-2\int_0^y \frac{m(z)}{v(z)}dz}$.

Therefore, under weak selection conditions, we can get

$$\begin{aligned} \phi_A\left(x\right) =& x + \frac{wN}{6k}x\left(1-x\right)\Bigg[\left(-2k^2+2k+1\right)\sum_{i=1}^{n}\pi_i Dr_i \\ &- \left(k^2-k+1\right)\sum_{i=1}^{n}\pi_i Dg_i + 3k \\ &+ \left(k^2-k-2\right)x\sum_{i=1}^{n}\pi_i\left(Dr_i - Dg_i\right)\Bigg]. \end{aligned} \tag{26}$$

E. Fixation Probability

According to Eq. (26), we yield the fixation probability ρ_A of a single A-individual in a population of $N-1$ B-individuals, which is given by

$$\begin{aligned} \rho_A =& \phi_A\left(\frac{1}{N}\right) = \frac{1}{N} + \frac{w}{6k}\left(1-\frac{1}{N}\right)\left[\left(-2k^2+2k+1\right)\right. \\ &\sum_{i=1}^{n}\pi_i Dr_i - \left(k^2-k+1\right)\sum_{i=1}^{n}\pi_i Dg_i + 3k \\ &\left.+ \frac{\left(k^2-k-2\right)}{N}\sum_{i=1}^{n}\pi_i\left(Dr_i - Dg_i\right)\right]. \end{aligned} \tag{27}$$

Therefore, for a sufficiently large population N, we obtain the condition under which natural selection favors strategy A, i.e., $\rho_A > 1/N$, which can be expressed as follows

$$3k > \left(2k^2-2k-1\right)\sum_{i=1}^{n}\pi_i Dr_i + \left(k^2-k+1\right)\sum_{i=1}^{n}\pi_i Dg_i. \tag{28}$$

■

II. Proof of Theorem 2

Based on Eq. (26), we can obtain the fixation probability ρ_B of a single B-individual in a population of $N-1$ A-individuals, which is given by

$$\begin{aligned} \rho_B =& 1 - \phi_A\left(\frac{N-1}{N}\right) = \frac{1}{N} - \frac{w}{6k}\left(1-\frac{1}{N}\right)\left[\left(-k^2+k-1\right)\right. \\ &\sum_{i=1}^{n}\pi_i Dr_i - \left(2k^2-2k-1\right)\sum_{i=1}^{n}\pi_i Dg_i + 3k \\ &\left.- \frac{k^2-k-2}{N}\sum_{i=1}^{n}\pi_i\left(Dr_i - Dg_i\right)\right]. \end{aligned} \tag{29}$$

Therefore, for a sufficiently large population N, we get the condition under which strategy B can be favored, i.e., $\rho_B > 1/N$, which can be expressed as follows

$$3k < \left(k^2-k+1\right)\sum_{i=1}^{n}\pi_i Dr_i + \left(2k^2-2k-1\right)\sum_{i=1}^{n}\pi_i Dg_i. \tag{30}$$

Based on Eqs. (27) and (29), we have the ratio of the fixation probabilities

$$\frac{\rho_A}{\rho_B} = 1 + w\frac{N-1}{2}\left[-\left(k-1\right)\sum_{i=1}^{n}\pi_i Dr_i - \left(k-1\right)\sum_{i=1}^{n}\pi_i Dg_i + 2\right]. \tag{31}$$

Consequently, for a sufficiently large population N, we derive the condition for strategy A to be favored over strategy B, i.e., $\rho_A > \rho_B$, which is given by

$$\sum_{i=1}^{n}\pi_i\left(Dr_i + Dg_i\right) < \frac{2}{k-1}. \tag{32}$$

■

III. Proof of Theorem 3

According to Eq. (8) of the main manuscript, to maximize the gradient of cooperation selection under two different games, we need to minimize $J_1(\pi_1) = \pi_1 G_1(p_A)$, subject to the constraint $\pi_1 + \pi_2 = 1$, where $G_1(p_A)$ is given by

$$\begin{aligned} G_1\left(p_A\right) =& \left(k^2-k-1\right)\left(Dr_1 - Dr_2\right) + \left(Dg_1 - Dg_2\right) \\ &- \left(k^2-k-2\right)\left(Dr_1 - Dg_1 - Dr_2 + Dg_2\right)p_A. \end{aligned} \tag{33}$$

Since $J_1(\pi_1)$ is a linear function of π_1, its optimal value is attained at either $\pi_1 = 1$ or $\pi_1 = 0$. To determine the optimal choice, we take the derivative of $G_1(p_A)$ and yield

$$G_1'\left(p_A\right) = -\left(k^2-k-2\right)\left(Dr_1 - Dg_1 - Dr_2 + Dg_2\right). \tag{34}$$

By substituting $p_A = 0$ and $p_A = 1$ into Eq. (33), we obtain

$$G_1(0) = \left(k^2 - k - 1\right)(Dr_1 - Dr_2) + (Dg_1 - Dg_2), \quad (35)$$

and

$$G_1(1) = \left(k^2 - k - 1\right)(Dg_1 - Dg_2) + (Dr_1 - Dr_2). \quad (36)$$

We first analyze the case where 1) $Dr_1+Dg_2 > Dg_1+Dr_2$. In this scenario, we have $G_1'(p_A) < 0$, which implies that $G_1(p_A)$ decreases as p_A grows.

(i) If $(k^2 - k - 1)(Dr_1 - Dr_2) + (Dg_1 - Dg_2) < 0$, then $G_1(p_A) < 0$ for any $p_A \in (0, 1)$ since $G_1(0) < 0$ and $G_1(p_A)$ decreases monotonically as p_A grows. In this case, the gradient of cooperation selection is maximized when $\pi_1 = 1$.

(ii) If $(k^2 - k - 1)(Dg_1 - Dg_2) + (Dr_1 - Dr_2) > 0$, then $G_1(p_A) > 0$ for any $p_A \in (0, 1)$ since $G_1(1) > 0$ and $G_1(p_A)$ decreases monotonically as p_A increases. In this case, the gradient of cooperation selection is maximized when $\pi_1 = 0$.

(iii) If $(k^2 - k - 1)(Dr_1 - Dr_2) + (Dg_1 - Dg_2) > 0$ and $(k^2 - k - 1)(Dg_1 - Dg_2) + (Dr_1 - Dr_2) < 0$, then there exists a point $p_A^* = [(k^2 - k - 1)(Dr_1 - Dr_2) + (Dg_1 - Dg_2)]/[(k^2 - k - 2)(Dr_1 - Dg_1 - Dr_2 + Dg_2)] \in (0, 1)$ such that $G(p_A^*) = 0$ since $G_1(0) > 0$, $G_1(1) < 0$, and $G_1(p_A)$ decreases monotonically as p_A grows. Therefore, $G_1(p_A) > 0$ always holds for $p_A \in (0, p_A^*)$, and the gradient of cooperation selection is maximized when $\pi_1 = 0$. In contrast, for $p_A \in [p_A^*, 1)$, $G_1(p_A) \leq 0$ always satisfies, and the gradient of cooperation selection is maximized when $\pi_1 = 1$.

Subsequently, we investigate the case where 2) $Dr_1 + Dg_2 < Dg_1 + Dr_2$. In this scenario, we have $G_1'(p_A) > 0$, which means that $G_1(p_A)$ increases as p_A grows.

(i) If $(k^2 - k - 1)(Dr_1 - Dr_2) + (Dg_1 - Dg_2) > 0$, then $G_1(p_A) > 0$ for any $p_A \in (0, 1)$ since $G_1(0) > 0$ and $G_1(p_A)$ increases monotonically as p_A grows. In this case, the gradient of cooperation selection is maximized when $\pi_1 = 0$.

(ii) If $(k^2 - k - 1)(Dg_1 - Dg_2) + (Dr_1 - Dr_2) < 0$, then $G_1(p_A) < 0$ for any $p_A \in (0, 1)$ since $G_1(1) < 0$ and $G_1(p_A)$ increases monotonically as p_A increases. In this case, the gradient of cooperation selection is maximized when $\pi_1 = 1$.

(iii) If $(k^2 - k - 1)(Dr_1 - Dr_2) + (Dg_1 - Dg_2) < 0$ and $(k^2 - k - 1)(Dg_1 - Dg_2) + (Dr_1 - Dr_2) > 0$, then there exists a point $p_A^* = [(k^2 - k - 1)(Dr_1 - Dr_2) + (Dg_1 - Dg_2)]/[(k^2 - k - 2)(Dr_1 - Dg_1 - Dr_2 + Dg_2)] \in (0, 1)$ such that $G_1(p_A^*) = 0$ since $G_1(0) < 0$, $G_1(1) > 0$, and $G_1(p_A)$ increases monotonically as p_A grows. Therefore, $G_1(p_A) < 0$ always holds for $p_A \in (0, p_A^*)$, and the gradient of cooperation selection is maximized when $\pi_1 = 1$. Conversely, for $p_A \in [p_A^*, 1)$, $G_1(p_A) \geq 0$ always satisfies, and thereby the gradient of cooperation selection is maximized when $\pi_1 = 0$. ■

IV. Proof of Theorem 4

Based on Eqs. (1) and (20), we can transform the optimization problem into minimizing $H_2(\Pi) = \sum_{i=1}^{n} [p_A (Dg_i - Dr_i) + Dr_i] \pi_i$. In the case of two different games, to minimize the fitness difference between defectors and cooperators, we need to minimize $J_2(\pi_1) = \pi_1 G_2(p_A)$, subject to the constraint $\pi_1 + \pi_2 = 1$, where $G_2(p_A)$ have the following form

$$G_2(p_A) = (Dg_1 - Dg_2)p_A + (Dr_1 - Dr_2)(1 - p_A). \quad (37)$$

We can get the optimal value of π_1 is either 1 or 0 since $J_2(\pi_1)$ is a linear function of π_1. To determine the optimal choice, we take the derivative of $G_2(p_A)$ and yield

$$G_2'(p_A) = Dg_1 - Dg_2 + Dr_2 - Dr_1. \quad (38)$$

By substituting $p_A = 0$ and $p_A = 1$ into Eq. (37), we have

$$G_2(0) = Dr_1 - Dr_2, \quad (39)$$

and

$$G_2(1) = Dg_1 - Dg_2. \quad (40)$$

We first analyze the situation of 1) $Dg_1+Dr_2 > Dg_2+Dr_1$, where we have $G_2'(p_A) > 0$, indicating that $G_2(p_A)$ increases as p_A grows.

(i) If $Dr_1 > Dr_2$, then $G_2(p_A) > 0$ for any $p_A \in (0, 1)$ since $G_2(0) > 0$ and $G_2(p_A)$ increases monotonically as p_A increases. In this case, the fitness difference between defectors and cooperators is minimized when $\pi_1 = 0$.

(ii) If $Dg_1 < Dg_2$, then $G_2(p_A) < 0$ for any $p_A \in (0, 1)$ since $G_2(1) < 0$ and $G_2(p_A)$ increases monotonically as p_A grows. In this case, the fitness difference between defectors and cooperators is minimized when $\pi_1 = 1$.

(iii) If $Dr_1 < Dr_2$ and $Dg_1 > Dg_2$, then there exists a point $p_A^* = (Dr_2 - Dr_1)/(Dg_1 - Dg_2 - Dr_1 + Dr_2) \in (0, 1)$ such that $G_2(p_A^*) = 0$ since $G_2(0) < 0$, $G_2(1) > 0$, and $G_2(p_A)$ increases monotonically as p_A increases. Therefore, $G_2(p_A) < 0$ always holds for $p_A \in (0, p_A^*)$, and the fitness difference between defectors and cooperators is minimized when $\pi_1 = 1$. In contrast, for $p_A \in [p_A^*, 1)$, $G_2(p_A) \geq 0$ always satisfies, and thereby the fitness difference between defectors and cooperators is minimized when $\pi_1 = 0$.

Subsequently, we investigate the situation of 2) $Dg_1 + Dr_2 < Dg_2 + Dr_1$, where we have $G_2'(p_A) < 0$, meaning that $G_2(p_A)$ decreases as p_A grows.

(i) If $Dr_1 < Dr_2$, then $G_2(p_A) < 0$ for any $p_A \in (0, 1)$ since $G_2(0) < 0$ and $G_2(p_A)$ decreases monotonically as p_A increases. In this case, the fitness difference between defectors and cooperators is minimized when $\pi_1 = 1$.

(ii) If $Dg_1 > Dg_2$, then $G_2(p_A) > 0$ for any $p_A \in (0, 1)$ since $G_2(1) > 0$ and $G_2(p_A)$ decreases monotonically as p_A grows. In this case, the fitness difference between defectors and cooperators is minimized when $\pi_1 = 0$.

(iii) If $Dr_1 > Dr_2$ and $Dg_1 < Dg_2$, then there exists a point $p_A^* = (Dr_2 - Dr_1)/(Dg_1 - Dg_2 - Dr_1 + Dr_2) \in (0, 1)$ such that $G_2(p_A^*) = 0$ since $G_2(0) > 0$, $G_2(1) < 0$, and $G_2(p_A)$ decreases monotonically as p_A grows. Therefore, $G_2(p_A) > 0$ always holds for $p_A \in (0, p_A^*)$, and the fitness difference between defectors and cooperators is minimized when $\pi_1 = 0$. Conversely, for $p_A \in [p_A^*, 1)$, $G_2(p_A) \leq 0$

always satisfies, and thereby the fitness difference between defectors and cooperators is minimized when $\pi_1 = 1$. ■

V. Further Numerical and Simulation Results for Optimization

In this section, we present additional numerical and simulation results about the optimization problems of (i) maximizing the gradient of cooperation selection and (ii) minimizing the fitness difference between defectors and cooperators. These results serve to validate the final three theoretical predictions stated in Thms. 3 and 4 of the main manuscript, respectively.

A. Further Numerical and Simulation Results for Maximizing the Gradient of Cooperation Selection

To validate the final three theoretical predictions regarding the maximization of the gradient of cooperation selection as demonstrated in Thm. 3 of the main manuscript, we provide corresponding numerical and simulation results for each of the three cases in Fig. 1. Specifically, the parameter settings for rows 1-3 in the figure satisfy $Dg_2 + Dr_1 < Dg_1 + Dr_2$, with $(k^2 - k - 1)(Dr_1 - Dr_2) + (Dg_1 - Dg_2) > 0$ for row 1, $(k^2 - k - 1)(Dg_1 - Dg_2) + (Dr_1 - Dr_2) < 0$ for row 2, and $(k^2 - k - 1)(Dr_1 - Dr_2) + (Dg_1 - Dg_2) < 0, (k^2 - k - 1)(Dg_1 - Dg_2) + (Dr_1 - Dr_2) > 0$ for row 3.

In Fig. 1(a), we observe that the gradient of selection corresponding to $\pi_1 = 0.0$ marked by blue circles is the highest across all values of cooperator frequency and decreases monotonically as π_1 increases. Fig. 1(b) shows that all scenarios ultimately lead to full cooperation, with $\pi_1 = 0.0$ achieving this most rapidly. As π_1 increases, the time required to reach full cooperation increases. These trends are further confirmed by the Monte Carlo simulation results in Fig. 1(c). In contrast, Fig. 1(d) demonstrates that the gradient of selection is maximized for $\pi_1 = 1.0$ marked by the green diamonds and decreases as π_1 decreases. This is corroborated by Fig. 1(e), which shows that cooperation emerges most quickly under $\pi_1 = 1.0$, whereas in the $\pi_1 = 0.0$ scenario, cooperators will eventually go extinct. These observations are again supported by the simulation results illustrated in Fig. 1(f). In Fig. 1(g), a threshold phenomenon is observed: when the cooperator frequency $x \in (0, x^*]$, where $x^* = [(k^2-k-1)(Dr_1-Dr_2)+(Dg_1-Dg_2)]/[(k^2-k-2)(Dr_1-Dg_1-Dr_2+Dg_2)]$, indicated by the orange vertical dashed line, the gradient of selection is largest at $\pi_1 = 1.0$; however, when $x \in (x^*, 1)$, it is maximized at $\pi_1 = 0.0$. Furthermore, both the numerical and simulation results presented in Figs. 1(h) and 1(i) demonstrate that, given a sufficiently long evolutionary time, the cooperator frequency under $\pi_1 = \pi_1^*$ always achieves the highest or reaches the full cooperation state fastest compared to the other cases, where π_1^* denotes the value of π_1 that maximizes the gradient of selection in Fig. 1(g). These results provide strong support for the theoretical predictions, with numerical and simulation outcomes in excellent agreement.

B. Further Numerical and Simulation Results for Minimizing the Fitness Difference between Defectors and Cooperators

To validate the final three theoretical predictions regarding the minimization of the fitness difference between defectors and cooperators as presented by Thm. 4 of the main manuscript, we provide corresponding numerical and simulation results for each of the three cases in Fig. 2. Concretely, the parameter settings satisfy $Dg_1 + Dr_2 < Dg_2 + Dr_1$, with $Dr_1 < Dr_2$ for row 1, $Dg_1 > Dg_2$ for row 2, and $Dr_1 > Dr_2, Dg_1 < Dg_2$ for row 3.

In Fig. 2(a), we observe that the fitness difference between defectors and cooperators is minimized at $\pi_1 = 1.0$ marked by green diamonds and increases monotonically as π_1 decreases. Fig. 2(b) further shows that all scenarios eventually reach the fully cooperative state, with the fastest convergence occurring at $\pi_1 = 1.0$. The time required to achieve full cooperation increases as π_1 decreases. These findings are corroborated by the Monte Carlo simulation results displayed in Fig. 2(c). Conversely, Fig. 2(d) shows that the fitness difference is minimized at $\pi_1 = 0.0$ indicated by blue circles and increases with increasing π_1. Analogously, Fig. 2(e) demonstrates that the fully cooperative state is reached most rapidly when $\pi_1 = 0.0$, a conclusion also supported by the simulation results shown in Fig. 2(f). In Fig. 2(g), we identify a critical threshold $x^* = (Dr_2 - Dr_1) / (Dg_1 - Dg_2 - Dr_1 + Dr_2)$ marked by the orange vertical dashed line. When the cooperator frequency $x \in (0, x^*]$, the fitness difference is smallest for $\pi_1 = 0.0$; in contrast, for $x \in (x^*, 1)$, the smallest fitness difference occurs at $\pi_1 = 1.0$. Furthermore, the numerical and simulation results depicted in Figs. 2(h) and 2(i) reveal that over a sufficiently long evolutionary period, the scenario with $\pi_1 = \pi_1^*$ achieves the highest number of cooperators or reaches full cooperation the fastest compared to the other cases, where π_1^* corresponds to the value of π_1 that minimizes the fitness difference in Fig. 2(g). Collectively, these results exhibit strong consistency between theoretical predictions and both numerical and simulation findings.

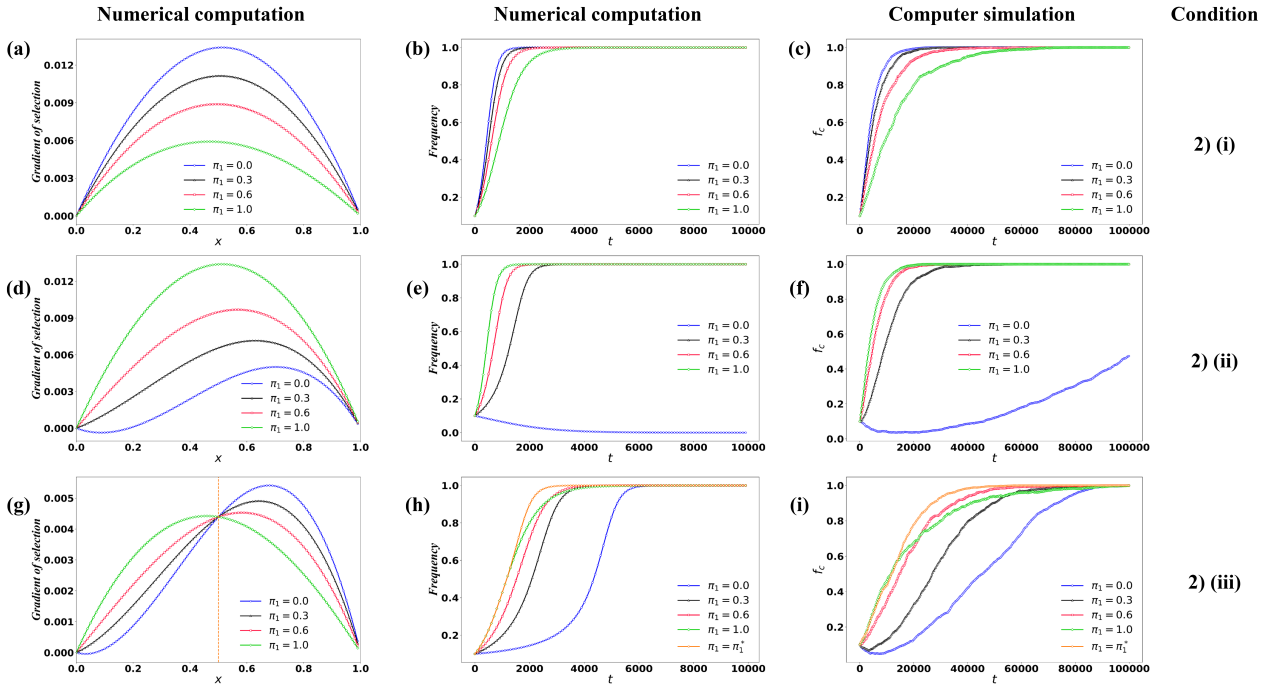

Fig. 1. **Numerical and simulation results for maximizing the gradient of cooperation selection.** The first column illustrates the numerical results of the gradient of cooperation selection as a function of the fraction of cooperators under different stationary game distributions. The second and third columns display the corresponding numerical and Monte Carlo simulation results, respectively, for the evolutionary trajectories of the cooperator frequency over time. Each row corresponds to a different theoretical case for maximizing the gradient of cooperation selection, as stated in items 2)(i)-(iii) of Thm. 3 in the main manuscript. The vertical orange dashed line in panel (g) denotes the critical point x^* at which $G_1(x^*) = 0$ shown in Eq. (33).

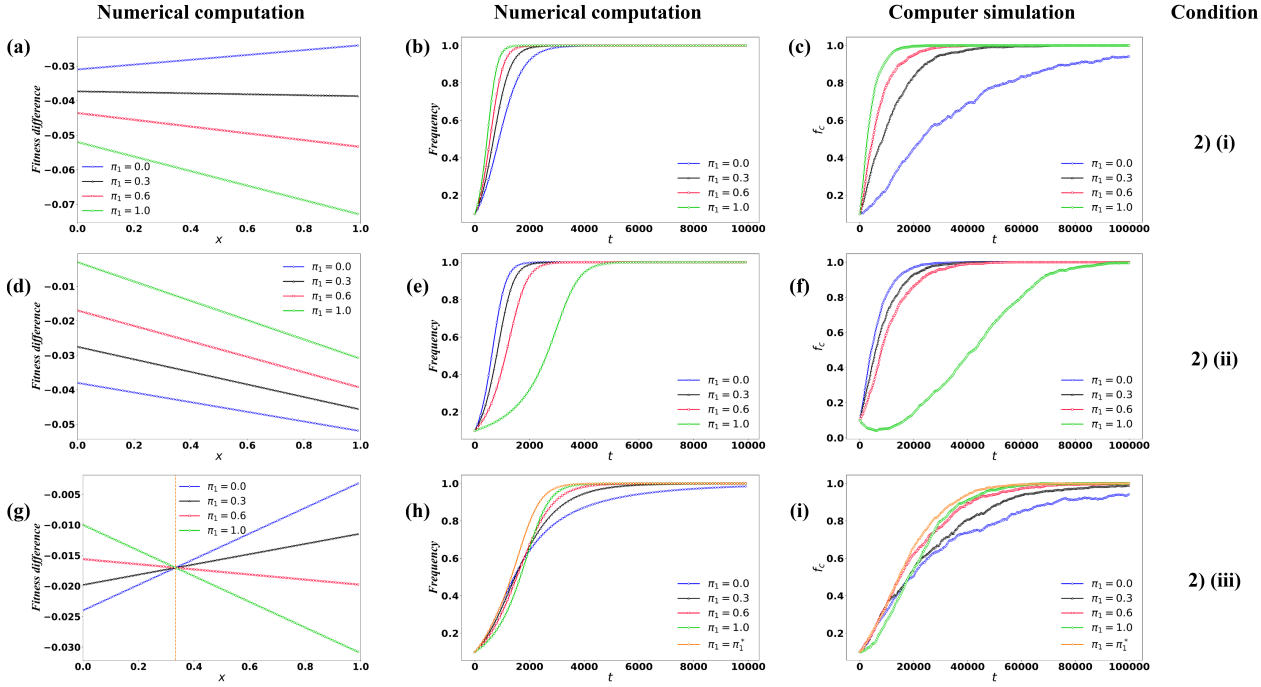

Fig. 2. **Numerical and simulation results for minimizing the fitness difference between defectors and cooperators.** The first column represents the numerical results of the fitness difference between defectors and cooperators as a function of the proportion of cooperators under different stationary game distributions. The second and third columns display the numerical and simulation results, respectively, for the evolutionary trajectories of the cooperator frequency over time under these distributions. Each row corresponds to a different theoretical case for minimizing the fitness difference between defectors and cooperators, as described in items 2)(i)-(iii) of Thm. 4 in the main manuscript. The vertical orange dashed line in panel (g) indicates the critical point x^* that makes $G_2(x^*) = 0$ presented in Eq. (37).